

AFOSR-TR. 88-1219

AIR FORCE OFFICE of SCIENTIFIC RESEARCH

ANNUAL REPORT

for period 30 June 1987 to 1 July 1988

GRANT NO. 85-0185

entitled

"II-VI SEMICONDUCTOR SUPERLATTICES"

by

Professor Robert L. Gunshor, Co-Principal Investigator
Professor Leslie A. Kolodziejski, Faculty Participant
School of Electrical Engineering
Professor Nobuo Otsuka, Co-Principal Investigator
Materials Engineering
Purdue University
West Lafayette, Indiana 47907



Accession For	
NTIS GRA&I	<input checked="" type="checkbox"/>
DTIC TAB	<input type="checkbox"/>
Unannounced	<input type="checkbox"/>
Justification	
By	
Distribution/	
Availability Codes	
Dist	Avail and/or Special
A-1	

OBJECTIVE

The objective of this research program is to study the kinetic growth processes involved in the molecular and atomic beam epitaxy of ZnSe, ZnSe alloys, and ZnSe-based multiple quantum wells. Monte Carlo studies of the growth processes are carried out in conjunction with selected experiments to determine various parameters necessary to provide a complete description of the growth modelling code. Complete understanding of the incorporation processes involved in the MBE growth will be necessary to succeed in controlling the carrier type in the wide bandgap II-VI semiconductor. Controlled substitutional doping of ZnSe, to contain both p- and n-type carriers, is also under investigation. Three main topics have been pursued during the course of the last year which include i) comparisons of Monte Carlo simulations and MBE growth experiments to describe the kinetic growth processes involved in the molecular beam epitaxy of ZnSe, ii) the controlled substitutional n-type doping of ZnSe with gallium, and iii) the isoelectronic delta doping of tellurium in ZnSe-based heterostructures fabricated by employing atomic layer epitaxy growth techniques; a summary of each major accomplishment is included below.

KINETIC GROWTH PROCESSES INVOLVED In the MBE OF ZnSe

The research on the growth modelling of MBE has been focussed on the incorporation processes in the growth of ZnSe, the control of which is considered to be one of the critical ingredients for achieving controlled doping of this wide bandgap material. For the experimental study, absolute measurements of the Zn and Se fluxes have been performed by three different methods: i) the deposition of Zn and Se on cold substrates, ii) the estimation by means of a quartz crystal monitor, and iii) the growth of ZnSe under Zn or Se over flux conditions. Based on the flux measurements, the flux ratio was set at exactly unity for the growth of (100) ZnSe at 320 °C. Under this condition, relatively high sticking coefficients of Zn and Se, and Se-rich growth surfaces are obtained. Monte Carlo simulations of the growth processes suggest that these experimental observations result from the following incorporation processes: Zn atoms arriving at the Se-covered surface and Se atoms arriving at the Zn-covered surface are incorporated into the ZnSe crystal with nearly unity sticking probabilities. In addition, appreciable portions of Se atoms arriving at the Se-covered surface are incorporated into the growing crystal through surface migrations of physisorbed atoms and molecules. A preprint of a paper, describing this work, presented at the Fifth International Conference on Molecular Beam Epitaxy in Sapporo, Japan this August, is included in

Appendix A; the publication will appear in the *Journal of Crystal Growth*.

In the past year, the main effort of the TEM group has been directed to the completion of the new high resolution electron microscope facility for the study of the MBE-grown structures. With the new JEM 2000 EX electron microscope, equipped with an ultrahigh resolution pole piece, we have obtained a point resolution of 2.1 Å. The facility also has a new ion milling machine which includes iodine source guns for preparation of damage-sensitive materials. Through the collaboration with Gatan, Inc. (The iodine guns are the first product of this company.), we have solved a number of problems caused by the usage of iodine, including degradation of the vacuum system and deposition of iodine on thin samples. With the capabilities of these new instruments, we have started the analysis of atomic structures of interfaces in II-VI semiconductor heterostructures. Besides the work with the MBE group at Purdue, the TEM group is continuing active collaborations with outside MBE groups represented by those of University of Illinois (Morkoç), North Carolina State University (Schetzina), Colorado State University (Robinson), Rockwell (Gerther), General Electric (Myers), and Hughes (Wu).

MBE GROWTH of ZnSe DOPED with GALLIUM

The II-VI compound semiconductor family, and the potential of these materials for device applications, have remained relatively untapped due to the substantial difficulties in preparing the II-VIs, by any growth technique, to contain both p-type carriers and n-type carriers. Bulk, liquid phase, or vapor phase growth techniques of the past used very high temperatures for the fabrication of ZnSe, and consequently control of the carrier type could not be achieved. The resultant ZnSe always exhibited n-type transport properties, or the as-grown material was so heavily compensated that the material was highly resistive. Newer growth technologies such as molecular beam epitaxy provide promise of circumventing the doping problems of the II-VIs, and ZnSe in particular, due to the non-equilibrium nature of the growth, and by the ability to affect the growth with photon illumination, for example.

Studies of dopant incorporation reported in the literature for ZnSe have been complicated by the presence of unintentional impurities found in both elemental and compound source material used in the MBE growth process. In most cases undoped ZnSe grown by MBE, using commercially available source material, has been reported to be n-type with low resistivity (~ 1 ohm-cm). The low resistivity of the "undoped" ZnSe material implied that the ZnSe was of good stoichiometry as a relatively small deviation from a unity Zn-to-Se flux ratio, toward either Zn-rich or Se-rich conditions, was found to result in high resistivity material. (The defects generated during growth under

non-stoichiometric conditions appeared to compensate the non-intentionally incorporated impurities giving rise to the high resistivity.) For example, in doping experiments performed in our laboratory, at a given Ga oven temperature, the resistivity was found to increase by two orders of magnitude when the flux ratio (Se/Zn) went from one to two. (The flux of each element was measured by a quartz crystal monitor placed in the approximate position of the substrate.) Through enhancement of the purity of the source material by vacuum distillation and/or zone-refining, nominally undoped ZnSe, grown under similar conditions of substrate temperature and flux ratio, exhibited high resistivity ($\sim 10^4$ ohm-cm). The use of purity-enhanced source material was reported by three groups. Yoneda et al. [*Appl. Phys. Lett.* 45, pp. 1300, 1984] performed a study in which they reported the variation of carrier concentration, resistivity, and relative intensity of free exciton emission for undoped ZnSe as a function of purification cycles, where the Se source material was vacuum distilled. The carrier concentrations ranged from 1×10^{17} cm $^{-3}$ to less than 7×10^{14} cm $^{-3}$ as the number of purification cycles was varied from 1 to 9, respectively.

At Purdue we have consistently used vacuum distilled source material (Zn, Se, Mn, and CdTe) prepared in-house for the growth of (Cd,Mn)Te, ZnSe, and (Zn,Mn)Se. In our case, depending on the conditions of the MBE apparatus and particular charge of source material, we have measured both high resistivity ($\sim 10^4$ ohm-cm) undoped ZnSe and lower resistivity undoped ZnSe (on the order of 3 ohm-cm). We have also grown undoped ZnSe using commercially available, vacuum distilled source material obtained from Osaka Asahi Mining Company. Again we found nominally undoped ZnSe to have a resistivity greater than 10^4 ohm-cm. The enhanced purity of the resultant ZnSe epilayers was confirmed in photoluminescence measurements where free exciton features were more prominent, having intensities similar to, and sometimes greater than, bound exciton related transitions. Our observations agreed with the results of Ohkawa et al. [K. Ohkawa, T. Mitsuyu, and O. Yamazaki, Extended Abstracts of the 18th Conference on Solid State Devices and Material, Tokyo, p.635, 1986] where they obtained high resistivity (10^4 ohm-cm) undoped ZnSe using the purity-enhanced source material purchased from the above commercial vendor. When intentionally incorporating Ga into ZnSe, we have obtained carrier concentrations of up to 2×10^{17} cm $^{-3}$ with room temperature mobilities of 200-400 cm 2 /V-sec. For epilayers of ZnSe:Ga a peak mobility of 7330 cm 2 /V-sec was obtained at 52K with a room temperature carrier concentration of 8×10^{14} cm $^{-3}$.

Successful incorporation of gallium into ZnSe has been achieved and the preprint of a paper describing the transport and optical properties of these MBE-grown layers

has been included in Appendix A. This preprint represents a paper presented at the Ninth Molecular Beam Epitaxy Workshop this August, 1988 and will appear in the *Journal of Vacuum Science and Technology*.

EXCITONIC TRAPPING BY ULTRATHIN LAYERS OF ATOMIC LAYER EPITAXIAL ZnTe WITHIN ZnSe-BASED HETEROSTRUCTURES

The difficulty in obtaining p-type ZnSe to serve as an injector of holes was the primary motivating factor leading to the growth of ZnSe/ZnTe superlattice structures. ZnTe is readily doped p-type while the Zn(Se,Te) alloy can be either n- or p-type depending on the Te fraction. There are however several potential difficulties associated with ZnSe/ZnTe heterostructures. The band offsets predicted by the electron affinity rule would suggest a Type II superlattice where holes and electrons are confined in separate layers. The resultant decrease in the oscillator strength of optical transitions could pose a problem for light emitting devices. A more serious consideration is the large lattice constant mismatch between ZnSe and ZnTe (7.4%); however, strained-layer superlattice structures are still possible with layer thicknesses restricted to a few tens of angstroms. For structures containing primarily ZnSe a reasonable lattice match to GaAs is still possible, whereas for structures containing approximately equal amounts of ZnSe and ZnTe, the average lattice constant approaches the lattice constant of InP. ZnSe/ZnTe superlattice structures have been grown at Purdue by a combination of ALE and MBE. Photoluminescence studies of the MBE-grown superlattice structures show a wide wavelength tunability as a function of the ratio of ZnSe to ZnTe layer thicknesses; photoluminescence emission is observed from the red to the green portion of the visible spectrum.

Specially designed ZnSe/ZnTe superlattice structures can also be viewed as a means to circumvent the difficulties encountered in the MBE growth of the Zn(Se,Te) alloy. Zn(Se,Te) is of particular interest due to the observation that the photoluminescence yield of the alloy can be significantly enhanced over that of bulk ZnSe crystals and epitaxial layers due to localization of excitons in the random alloy. The growth of the Zn(Se,Te) mixed crystal by molecular beam epitaxy however, is complicated by a difficulty in controlling the composition. In the work reported by Yao et al. [*J. Crystal Growth* 45:309 (1978)], over the entire range of Te fraction, a Te-to-Se flux ratio of 3 to 10 was required. In our laboratory we have grown a number of Zn(Se,Te) epilayers with varying fractions of Te; a particular difficulty was encountered when a small fraction of Te was desired, resulting in widely varying compositions under what appeared to be similar growth conditions. To circumvent the problems associated with

controlling the alloy concentrations, we have designed ZnSe-based structures consisting of ultrathin layers of ZnTe spaced by appropriate dimensions to approximate a Zn(Se,Te) mixed crystal with low or moderate Te composition.

As an illustration, such a "pseudo-alloy" was used to modify the ZnSe quantum well in a ZnSe/(Zn,Mn)Se heterostructure. In these multiple quantum well structures either one or two ZnTe sheets were placed in the center of each ZnSe well; the well thicknesses ranged from 44 to 130 Å. In an effort to optimize the interface abruptness of the ZnTe monolayers, the ALE of ZnTe was performed on a recovered ZnSe surface which made up, for example, the first half of a quantum well, whereas the remainder of the structure was grown by MBE. Although the architecture of these structures was substantially different from a bulk alloy, their optical transitions as viewed in photoluminescence were dominated by features which were quite similar to those found in the bulk alloy crystals at low to moderate Te composition. Figure 1 dramatically illustrates exciton trapping at the ZnTe monolayer sheets present in the ZnSe quantum well. For comparison purposes Figure 1(a) shows the low temperature photoluminescence spectrum of a ZnSe/(Zn,Mn)Se MQW structure. The luminescence was dominated by the sharp (FWHM < 5 meV), bright, blue exciton recombination at the $n=1$ (light hole) quantum well transition. As a striking contrast to Figure 1(a) the photoluminescence from a ZnSe/(Zn,Mn)Se MQW, which now incorporates the ZnTe "sheets" inserted into each quantum well, is shown in Figure 1(b). The broad luminescence features at lower energy were the result of exciton localization at the ZnTe/ZnSe heterointerfaces and were similar to those seen from bulk Zn(Se,Te) mixed crystals. Figure 1(c), showing a photoluminescence excitation (PLE) spectrum, indicates that the position of the lowest energy exciton transition has not been significantly shifted by the presence of the ZnTe sheets. These first research results are detailed in the *Applied Physics Letters* reprint included in Appendix A of this report. Further optical and magneto-optical studies on structures containing Mn provided conclusive evidence that the Te sites provided a trap for the hole part of the exciton, increasing the exciton's lifetime from 200 psec to 50 nsec. Many additional ZnSe-based heterostructures containing ultrathin sheets of ZnTe have been grown and are currently under investigation to study the mechanism of the excitonic self-trapping.

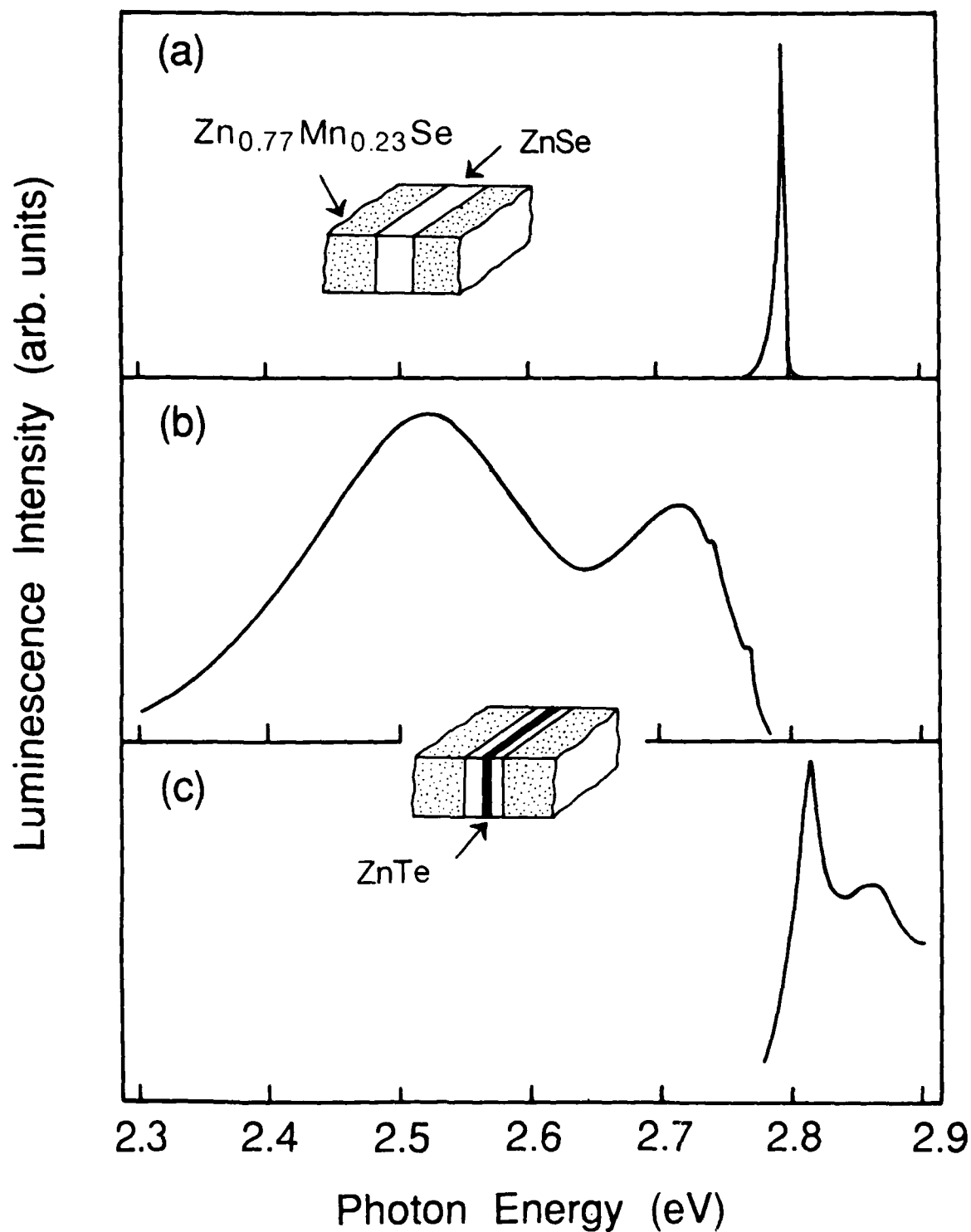


Figure 1: Comparison of photoluminescence spectra at $T=2\text{K}$: (a) ZnSe/(Zn,Mn)Se multiple quantum well sample, (b) a structure similar to that of (a) but with the insertion of a monolayer sheet of ZnTe in the middle of the quantum well (The amplitude of emission in (a) has been reduced to bring peak to scale.), (c) the photoluminescence excitation spectrum of sample (b) is shown in bottom panel.

PUBLICATIONS

A. INVITED BOOK CHAPTERS

*[1] R. L. Gunshor, L. A. Kolodziejski, N. Otsuka, and A. V. Nurmikko, "Semimagnetic and Magnetic Semiconductor Superlattices," in: *Annual Review of Materials Science*, Volume 18, pp. 247-253, 1988.

*[2] L. A. Kolodziejski, R. L. Gunshor, N. Otsuka, and A. V. Nurmikko, "MBE of Wide Bandgap II-VI Compound Semiconductor Superlattices and Diluted Magnetic Semiconductors," in: *Molecular Beam Epitaxy*, (eds. Robin F. C. Farrow and John R. Arthur), pp. xxx, 1988.

B. INVITED PUBLICATIONS

*[1] L. A. Kolodziejski, R. L. Gunshor, A. V. Nurmikko, and N. Otsuka, "II-VI/III-V Heterointerfaces: Epilayer on Epilayer Structures," *Mat. Res. Soc. Symp. Proc.* vol. 102, pp. 149-155, 1988.

*[2] R. L. Gunshor and L. A. Kolodziejski, "Recent Advances in the Molecular Beam Epitaxy of ZnSe and its Superlattices," *IEEE Trans. on Quantum Electronics* vol. QE-24, pp. 1744-1757, 1988.

C. SERIAL JOURNAL PUBLICATIONS

[1] T. C. Bonsett, M. Yamanishi, S. Datta, L. A. Kolodziejski, and R. L. Gunshor, "Polarization Dependent Optical Absorption and Gain Spectra of (Cd,Mn)Te and (Zn,Mn)Se Multiple Quantum Well Structures," *Applied Physics Letters*, pp. 499-501, 1987.

[2] E. K. Suh, D. U. Bartholomew, A. K. Ramdas, S. Rodriguez, S. Vanugopalan, L. A. Kolodziejski, and R. L. Gunshor, "Raman Scattering from Superlattices of Diluted Magnetic Semiconductors," *Physical Review B*, vol. 36, pp. 4316-4331, 1987.

- *[3] S. K. Chang, D. Lee, H. Nakata, A. V. Nurmikko, L. A. Kolodziejski, and R. L. Gunshor, "Frustrated Antiferromagnetism at the Heterointerfaces in a Semiconductor Superlattice: MnSe/ZnSe," *Journal of Applied Physics*, vol. 62, pp. 4835-4838, 1987.
- [4] Qiang Fu, A. V. Nurmikko, L. A. Kolodziejski, and R. L. Gunshor, "Electric Field Induced Shifts in Exciton Luminescence in ZnSe/(Zn,Mn)Se Superlattices," *Applied Physics Letters*, 51, pp. 578-580, 1987.
- [5] S. K. Chang, N. Nakata, A. V. Nurmikko, R. L. Gunshor, and L. A. Kolodziejski, "Resonant Raman Scattering and Exciton-Optical Phonon Coupling in CdTe/(Cd,Mn)Te Quantum Wells," *Applied Physics Letters*, 51, pp. 667-669, 1987.
- [6] S. K. Chang, A. V. Nurmikko, J. W. Wu, L. A. Kolodziejski, and R. L. Gunshor, "Bandoffsets and Excitons in CdTe/(Cd,Mn)Te Quantum Wells," *Physical Review B*, vol. 37, pp. 1191-1198, 1988.
- *[7] G. D. Studtmann, R. L. Gunshor, L. A. Kolodziejski, M. R. Melloch, J. A. Cooper, R. F. Pierret, D. P. Munich, C. Choi, and N. Otsuka, "Pseudomorphic ZnSe/n-GaAs Doped-Channel Field Effect Transistors by Interrupted MBE Growth," *Applied Physics Letters*, vol. 52, pp. 1249-1251, 1988.
- *[8] L. A. Kolodziejski, R. L. Gunshor, Q. Fu, D. Lee, A. V. Nurmikko, J. M. Gonsalves, and N. Otsuka, "Excitonic Trapping from Atomic Layer Epitaxial ZnTe Within ZnSe/(Zn,Mn)Se Heterostructures," *Applied Physics Letters*, vol. 52, pp. 1080-1082, 1988.

D. INVITED PRESENTATIONS

- [1] A. V. Nurmikko, S. K. Chang, D. Lee, A. Mysyrowicz, Q. Fu, L. A. Kolodziejski, and R. L. Gunshor, "Excitons and Nonlinear Optical Effects in II-VI Compound Semiconductor Quantum Wells," presented at the *Annual Optical Society Meeting*, Rochester, NY, October, 1987.
- *[2] L. A. Kolodziejski and R. L. Gunshor, "II-VI/III-V Heterostructures," presented at

the *Materials Research Society Meeting*, Boston, December, 1987.

*[3] L. A. Kolodziejski, "Molecular Beam Epitaxy Of Wide Bandgap II-VI Superlattices," presented at the *Maryland Institute of Materials*, Baltimore, February, 1988.

*[4] L. A. Kolodziejski, R. L. Gunshor, A. V. Nurmikko, and N. Otsuka, "Artificially Layered Structures Composed of Diluted Magnetic Semiconductors, presented at the *Greater New York American Vacuum Society Meeting*, Princeton, NJ, March, 1988.

*[5] L. A. Kolodziejski, R. L. Gunshor, N. Otsuka, and A. V. Nurmikko, "DMS Strained-Layer Superlattices," presented at the *Workshop on II-VI Semiconductors*, Karlsruhe, West Germany, March, 1988.

[6] D. Lee, A. V. Nurmikko, L. A. Kolodziejski, and R. L. Gunshor, "Transient Electronic Phenomena in a Highly Excited II-VI Compound Semiconductor Quantum Well," presented at the *SPIE Conference on Quantum Wells*, Newport Beach, March 1988.

*[7] L. A. Kolodziejski, R. L. Gunshor, N. Otsuka, and A. V. Nurmikko, "II-VI/III-V Heterointerfaces: Epilayer-on-Epilayer Structures," presented at the *Southwest Regional American Vacuum Society Meeting*, Albuquerque, NM, April, 1988.

*[8] A. V. Nurmikko, R. L. Gunshor, and L. A. Kolodziejski, "Strong Coupling of Phonons and Excitons in Semiconductor Superlattices: The Case of ZnSe/ZnTe Heterostructures," presented at the *International Conference on Quantum Electronics*, Tokyo, July, 1988.

*[9] Q. Fu, D. Lee, A. V. Nurmikko, L. A. Kolodziejski, and R. L. Gunshor, "Exciton Capture with Strong Lattice Relaxation in ZnSe/ZnTe Heterostructures," presented at the *International Conference on the Physics of Semiconductors*, Warsaw, July, 1988.

*[10] L. A. Kolodziejski, R. L. Gunshor, A. V. Nurmikko, and N. Otsuka, "Wide Gap II-VI Superlattices: MBE Growth and Characterization," presented at the *NATO Advanced Workshop on Wide Bandgap II-VI Semiconductors*, Regensburg, West Germany, August, 1988.

*[11] R. L. Gunshor, L. A. Kolodziejski, A. V. Nurmikko, and N. Otsuka, "II-VI-III-V Heterostructures: Epilayer-on-Epilayer Structures," presented at the *NATO Advanced Workshop on Wide Bandgap II-VI Semiconductors*, Regensburg, West Germany, August, 1988.

*[12] R. L. Gunshor, L. A. Kolodziejski, and A. V. Nurmikko, "ZnSe/MnSe Magnetic Semiconductor Superlattices," presented at the *Warren E. Henry Symposia*, Washington, D. C., August, 1988.

*[13] A. V. Nurmikko, R. L. Gunshor, and L. A. Kolodziejski, "Optical Characterization of Wide Bandgap II-VI Multiple Quantum Wells," presented at the *5th International Conference on Molecular Beam Epitaxy*, Sapporo, Japan, August, 1988.

E. CONFERENCE PRESENTATIONS

*[1] D. Lee, S. K. Chang, H. Nakata, A. V. Nurmikko, L. A. Kolodziejski, and R. L. Gunshor, "Magnetic and Electronic Properties of MnSe/ZnSe Superlattices Near the Monolayer Limit," presented at the *3rd International Conference on Modulated Semiconductor Structures*, July 6-10, 1987, Montpellier, France.

[2] S. K. Chang, N. Nakata, A. V. Nurmikko, L. A. Kolodziejski, and R. L. Gunshor, "Resonant Raman Scattering and Exciton-Phonon Interaction in CdTe/(Cd,Mn)Te Superlattices," presented at the *3rd International Conference on Modulated Semiconductor Structures*, July 6-10, 1987, Montpellier, France.

*[3] D. Lee, S. K. Chang, H. Nakata, A. V. Nurmikko, L. A. Kolodziejski, and R. L. Gunshor, "Influence of Interfaces on Electronic and Magnetic Properties of MnSe/ZnSe Superlattice near the Monolayer Limit," presented at the *3rd International Conference on Modulated Semiconductor Structures*, July 6-10, 1987, Montpellier, France.

*[4] G. D. Studtmann, R. L. Gunshor, L. A. Kolodziejski, M. R. Melloch, N. Otsuka, D. P. Munich, J. A. Cooper, and R. F. Pierret, "Pseudomorphic ZnSe/GaAs MISFET Devices," presented at the *45th Device Research Conference*, Santa Barbara, CA June 22-24, 1987.

*[5] C. Choi, N. Otsuka, L. A. Kolodziejski, and R. L. Gunshor, "Misfit Dislocations in the ZnSe/GaAs Heterostructure grown by Molecular Beam Epitaxy," presented at the *TMS Electronic Device Materials Meeting*, Phoenix, January, 1988.

*[6] M. Vaziri, R. Feifenberger, L. A. Kolodziejski, R. L. Gunshor, and R. Holzer, "Electrical and Optical Characterization of Ga-doped MBE grown ZnSe," presented at the

American Physical Society Meeting, New Orleans, March, 1988.

[7] Q. Fu, D. Lee, A. Mysyrowicz, A. V. Nurmikko, L. A. Kolodziejski, and R. L. Gunshor, "Observation of Excitonic Molecules in ZnSe/(Zn,Mn)Se Quantum Wells," presented at the *American Physical Society Meeting, New Orleans, March, 1988.*

[8] A. V. Nurmikko, D. Lee, P. Hawrylak, L. A. Kolodziejski, and R. L. Gunshor, "Electron-Hole Plasma and Exciton Screening in CdTe/(Cd,Mn)Te Quantum Wells," presented at the *American Physical Society Meeting, New Orleans, March, 1988.*

*[9] D. Lee, Q. Fu, A. V. Nurmikko, L. A. Kolodziejski, and R. L. Gunshor, "Exciton Self-Trapping in ZnSe/ZnTe Heterostructures," presented at the *American Physical Society Meeting, New Orleans, March, 1988.*

[10] A. Mysyrowicz, D. Lee, Q. Fu, A. V. Nurmikko, R. L. Gunshor, and L. A. Kolodziejski, "Biexcitons in ZnSe Based Quantum Wells," presented at the *International Conference on the Physics of Semiconductors, Warsaw, July, 1988.*

*[11] D. Lee, Q. Fu, A. V. Nurmikko, L. A. Kolodziejski, and R. L. Gunshor, "Widely Tunable Exciton Radiative Recombination Rate in ZnSe Based Superlattice Structures," presented at the *International Conference on Superlattices, Microstructures, and Microdevices, Trieste, Italy, August, 1988.*

[12] J. L. Glenn, Sungki O, L. A. Kolodziejski, R. L. Gunshor, M. Kobayashi, J. M. Gonsalves, N. Otsuka, M. Haggerott, T. Heyen, and A. V. Nurmikko, "MBE of InSb/CdTe Heterostructures," presented at the *5th International Conference on Molecular Beam Epitaxy, Sapporo, Japan, August, 1988.*

*[13] Q. D. Qian, J. Qiu, R. L. Gunshor, L. A. Kolodziejski, R. L. Gunshor, M. Kobayashi, M. R. Melloch, J. A. Cooper, "Passivation of Epitaxial GaAs with Epitaxial ZnSe," presented at the *5th International Conference on Molecular Beam Epitaxy, Sapporo, Japan, August, 1988.*

*[14] R. Venkatasubramanian, J. Qiu, N. Otsuka, L. A. Kolodziejski, and R. L. Gunshor, "Growth Processes of ZnSe grown by Molecular Beam Epitaxy," presented at the *5th International Conference on Molecular Beam Epitaxy, Sapporo, Japan, August, 1988.*

* Research supported by the Air Force Office of Scientific Research in conjunction with Office of Naval Research, and Defense Advanced Research Projects Agency.

F. GRADUATE DEGREES AWARDED

- R. Venkatasubramanian, Doctor of Philosophy, Purdue University, August, 1988
Thesis Title: Monte Carlo Simulation of the Kinetic Growth Processes of ZnSe grown by Molecular Beam Epitaxy

APPENDIX A

INCORPORATION PROCESSES IN MBE GROWTH OF ZnSe

R. Venkatasubramanian⁽¹⁾, N. Otsuka⁽²⁾, J. Qui⁽¹⁾
L. A. Kolodziej⁽¹⁾, and R. L. Gunshor⁽¹⁾

(1) School of Electrical Engineering

(2) School of Materials Engineering

Purdue University, W. Lafayette, IN 47907, USA

ABSTRACT

Absolute measurements of Zn and Se fluxes employed in MBE growth of ZnSe have been performed by using three different methods, the deposition of Zn or Se on cold substrates, the estimation by a quartz crystal monitor, and the growth of ZnSe under the Zn or Se over-flux conditions. Based on the results of the flux measurements, the flux ratio was set at unity in the growth of (100) ZnSe at 320°C. Under this condition, the growth surface exhibits a (2x1) structure, and high sticking coefficients of Zn and Se were obtained. A model of incorporation processes of Zn and Se in MBE growth of (100) ZnSe is proposed.

In recent years, major efforts of molecular beam epitaxy (MBE) of ZnSe are directed to the growth of low resistivity p-type epilayers. One of the main requirements in achieving this goal is the growth of stoichiometric epilayers which have sufficiently low concentrations of native defects for the controlled doping. Although the condition for the growth of high quality single crystalline ZnSe has been fairly well established to date, the condition for the growth of highly stoichiometric epilayers has not been closely investigated. Stoichiometry of epilayers is considered to be most directly affected by the ratio of Zn and Se fluxes among a number of growth parameters in MBE of ZnSe. In an earlier study [1], Yao et al. have investigated the dependence of the growth rate of (100) ZnSe on the flux ratio. Recently, Menda et al. [2], DePuydt et al. [3], and Cornelissen et al. [4] have studied surface structures of (100) epilayers by reflection high energy electron diffraction (RHEED) for various flux ratios and growth temperatures. Based on these observations, they have made surface phase diagrams in order to search for the optimum growth condition. In the experiments mentioned above (except those by Yao et al. [1]), beam pressures of Zn and Se fluxes were measured by means of an ionization gage, and the ratio of beam pressures was used as a substitute for the actual flux ratio, which is defined as the ratio of numbers of Zn and Se atoms impinging on the unit area of a substrate for the unit period of time. In general, a beam pressure ratio determined by an ionization gauge does not coincide with a flux ratio because of different relative sensitivities of atoms and molecules to ionization. In this case, particularly, it is extremely difficult to relate a beam pressure ratio to a flux ratio due to the evaporation of various forms of molecules from an elemental Se source [5].

In the present study, we have made absolute measurements of Zn and Se fluxes by employing three different methods. The first method is the measurement of thicknesses of Zn or Se layers deposited on cold substrates. The second method is the growth of ZnSe epilayers under Zn over-flux or Se over-flux conditions; from the thicknesses of the epilayers, fluxes of minority elements have been estimated. The third method is the measurement of fluxes by a quartz crystal monitor. Unlike an ionization gauge, a quartz crystal monitor can directly read a flux by measuring weight of the material deposited on the crystal monitor. Although each of three methods enables direct measurements of fluxes, their results have some ambiguities such as the possibility of non-unity sticking coefficients of Zn or Se. Therefore, the comparison of fluxes determined by different methods has been made for each deposition experiment. Based on the results of the flux measurements, we have set the flux ratio at unity for the growth of a ZnSe epilayer at 320°C. Sticking coefficients of Zn and Se and RHEED patterns of growing surfaces have been investigated for this condition. Based on results of the growth experiments, a model of incorporation processes in MBE of (100) ZnSe is proposed. For the experiments, a Perkin-Elmer model 400 MBE system has been used. Details of the procedure of the growth of ZnSe with this system are described in earlier reports [6,7].

Zn and Se were separately deposited on (100) GaAs substrates which were kept in contact with the liquid nitrogen shroud. Although actual temperatures of the substrates were not determined, they are

believed to be low enough to yield nearly unity sticking coefficients of Zn and Se. In order to enhance the sticking, besides the cooling, surfaces of GaAs were roughened by etching with a solution, 1 HCl: 1 CH₃COOH: 1 H₂O₂ for 2 minutes. The individual depositions of Zn and Se were carried out for 4 hours each, with effusion cell temperatures of 305°C and 183°C, respectively. Thicknesses of layers were measured by scanning electron microscope (SEM) observations of cross-sectional samples which were prepared by cleavage, mechanical polishing and Ar ion milling. Four areas on smooth substrate surfaces were chosen in each sample for the measurement of layer thicknesses. The SEM images show dense and fairly uniform layers in all observed areas. Densities of layers are assumed to be the same as those of bulk Zn and Se crystals. Table 1 lists Zn and Se fluxes estimated by this method. Errors of the values correspond to variations of layer thicknesses among four areas.

Before and after the deposition of Zn and Se on cold GaAs substrates, each flux was measured by a quartz crystal monitor. The crystal monitor was positioned close to the substrates position and kept at room temperature by water cooling. Flux reading changed from the start of the deposition to the end of the deposition by 5 to 10%. The average values of initial and final reading were used for the estimation of fluxes impinging on the substrates. Effects of the difference in position between the substrates and the monitor with respect to the Zn or Se effusion cells were corrected by utilizing the equation for the free molecular flow of a gas from an orifice under the condition of Langmuir evaporation [8]. Results of the estimation are listed in Table 1.

The method which employs the crystal monitor has two possible sources of underestimation of a flux impinging on the substrate. The first source is the significant deviation of the angular distribution of the flux from those of Langmuir evaporation, which may be caused by a large drop of the charge level of a source material from the level of the cell opening. The substrates were positioned on the center lines of both Zn and Se effusion cells, while angles between lines connecting the crystal monitor to the Zn and Se effusion cells and their center lines were 12.0° and 13.2°, respectively. In order to minimize errors caused by this effect, these experiments were performed with nearly identical charge levels of source materials which were kept close to the level of the cell openings by recharging the source materials in the effusion cells before experiments. The second source of underestimation is the possibility of non-unity sticking of Zn or Se on the crystal monitor. It is seen from Table 1 that fluxes estimated by the crystal monitor are close to those estimated by the method of deposition on cold substrates. Their differences are less than 8%. The close agreement suggests that neither effects explained above are significant under the condition employed in these experiments.

ZnSe epilayers were grown under conditions of either Zn over-flux or Se over-flux. The growth temperature was 320°C, and (100) GaAs crystals were used as substrates. Under the over-flux condition, that is, the flux of one element is far greater (~ 10:1) than that of the other element, atoms and molecules of the minority element are expected to be incorporated into the growing crystal with a nearly unity sticking coefficient. From the thickness of the ZnSe epilayer, therefore, one can estimate an absolute value of a flux of the minority element. The ZnSe epilayer was etched off to create a step in the epilayer by selective etching. By using a 100 Tencor surface profile-meter, the thickness of the epilayer was measured at several different locations along the step. Flux values estimated by this method are listed in Table 2, along with those estimated from reading of the quartz crystal monitor. As seen in Table 2, fluxes estimated by the two methods are close to each other, with differences of less than 8%. The agreement between these results suggests that reliable value of flux can be determined by using the quartz crystal monitor.

A ZnSe epilayer was grown at 320°C on (100) GaAs substrate with Se to Zn flux ratios of 1.0. The charge level of source materials in effusion cells were kept close to the cell opening for this growth. Temperatures of Zn and Se effusion cells were set at 300°C and 182°C, respectively. Fluxes impinging on substrates were estimated by using the quartz crystal monitor, corrected for the actual position of the crystal monitor, as described above. The growth rate of the epilayer was estimated from the thickness of the epilayer which was measured by the surface profile meter with selective etching. Zn and Se fluxes employed in the growth were $(3.0 \pm 0.1) \times 10^{14}$ atoms/cm² sec, and the growth rate was estimated as 0.85 ± 0.04 Å/sec. These values yield fairly high sticking coefficients for Zn and Se, 0.64 ± 0.04 . These sticking coefficients are greater than the values expected from the kinetic model which was employed in earlier studies of MBE growth of zinc chalcogenides [1,9,10]. In the kinetic model, it is assumed that sticking probabilities of Zn on a Se covered surface and Se on a Zn covered surface are unity, while those of Zn on a Zn covered surface and Se on a Se covered surface are assumed to be zero. Sticking coefficients of Zn and Se which were calculated based on the model are 0.5 for the flux ratio of

1.0). The differences between experimental and calculated values are greater than the errors of the measurements. Therefore, this result suggests that a portion of Zn arriving at Zn covered surfaces, or a portion of Se arriving at Se covered surfaces are incorporated into the growing crystal through surface migration. In an earlier study of MBE growth of (100) ZnSe, Yao et al. [1] estimated sticking coefficients of Zn and Se for the growth temperature of 350°C by using a quartz crystal monitor; their results agreed with the kinetic model, unlike the present case.

RHEED patterns in the [010], [001], [011] and $[0\bar{1}1]$ directions were observed during the growth of the epilayer. Observed RHEED patterns have shown the presence of a (2x1) structure. Fig. 1 are the [011] and [010] patterns taken from the epilayer. The [011] pattern shows distinct half order reflections, while no fractional order reflection is seen in the [010] pattern. The (100) surface of ZnSe is known to exhibit either a (2x1) structure or a c(2x2) structure during the MBE or atomic layer epitaxy (ALE) growth [2,3,4,11]. The former forms under the Se over-flux condition, while the latter appears under the Zn over-flux condition. RHEED observations made recently by other groups [2,3,4] show the presence of the c(2x2) structure on the (100) ZnSe surface with the beam pressure ratio of 1.0 at growth temperatures close to 320°C. From the observations of the epilayer, however, we did not find the c(2x2) structure during the growth. Only the (2x1) structure was seen in RHEED patterns. We have grown a number of (100) ZnSe epilayers at 320°C under similar conditions of flux ratios. In all these growth experiments, only the (2x1) structure has been observed during the growth of epilayers.

The following model can be suggested for incorporation processes of MBE growth of (100) ZnSe based on the observations made in this study. If we assume that the (2x1) structure occurs only on Se covered surfaces and that the c(2x2) structure is characteristic to Zn covered surfaces, our RHEED observations can be interpreted as follows. The majority of the growing surface is covered by Se when the flux ratio close to unity is employed in the growth. With this interpretation, one can explain high sticking coefficients of Zn and Se by the following incorporation processes. Zn atoms arriving at Se covered surfaces and Se atoms or molecules arriving at Zn covered surfaces are incorporated into the crystal with nearly unity sticking probabilities. In addition, appreciable portions of Se atoms or molecules arriving at a Se covered surface are also incorporated into the crystal through fast surface migration, which yields high sticking coefficients of Se as well as a large area of Se covered surfaces throughout the growth. The high sticking coefficient of Zn results simply from the large area of Se covered surfaces.

In order to examine the incorporation processes, Monte Carlo simulations of MBE growth of (100) ZnSe under the condition of the unity flux ratio have been performed. The basic framework of the simulation model is explained in an earlier paper [12]. Growth parameters such as flux and substrate temperature are set at experimental values. The fast surface migration of weakly bonded Se is included in the model by giving certain probabilities to Se atoms on Se covered surface to reach areas of Zn covered surfaces. With the inclusion of this process, simulations yield sticking coefficients close to 0.64 for both Zn and Se. Fig. 2 shows the coverage profiles of Zn and Se layers as a function of growth time. The spacings between Zn and Se coverage profiles along the axis of growth time directly corresponds to time periods during which Zn or Se covered surfaces are exposed to vacuum. From the figure, it is seen that the growth front of the crystal is covered by Se for about 60% of the growth period. Therefore, the results of simulation can explain the dominance of the (2x1) structure in observed RHEED patterns. Details of these simulations will be presented in a separate report.

The authors would like to thank Y. E. Ihm for his contribution to this work. The work was supported by a Air Force Office of Scientific Research grant No. 85-0185 and a Defense Advanced Research Project Agency/Office of Naval Research, University Research Initiative Program N00014-86-K0760.

REFERENCES

1. T. Yao, Y. Miyoshi, Y. Makita and S. Maekawa, Japan J. Appl. Phys. 16 (1977) 369.
2. K. Menda, I. Takayasu, T. Minato, and M. Kawashima, Japan J. Appl. Phys. 26 (1987) 1326.
3. J. M. DePuydt, H. Cheng, J. E. Potts, T. L. Smith, and S. K. Mohapatra, J. Appl. Phys. 62 (1987) 4756.

4. H. J. Cornelissen, D. A. Cammack, and R. J. Dalby, *J. Vac. Sci. Technol. B6* (1988) 769.
5. R. E. Honig and D. A. Kramer, *RCA Review*, 30 (1969) 285.
6. L. A. Kolodziejski, R. L. Gunshor, T. C. Bonsett, R. Venkatasubramanian, S. Datta, R. B. Bylsma, W. M. Becker, and N. Otsuka, *Appl. Phys. Lett.* 47 (1985) 169.
7. R. L. Gunshor, L. A. Kolodziejski, M. R. Melloch, M. Vaziri C. Choi and N. Otsuka, *Appl. Phys. Lett.* 50 (1987) 200.
8. L. I. Maissal and R. Clang, *Handbook of Thin Film Technology* (McGraw-Hill, 1970).
9. F. Kitagawa, T. Mishima, and K. Takahashi, *J. Electrochem. Soc.* 127 (1980) 937.
10. T. Yao and S. Maekawa, *J. Crystal Growth* 53 (1981) 423.
11. T. Yao and T. Takeda, *Appl. Phys. Lett.* 48 (1986) 160.
12. R. Venkatasubramanian, N. Otsuka, S. Datta, L. A. Kolodziejski, and R. L. Gunshor, *Proceedings of SPIE*, Vol. 796 (1987) 121.

Table 1. Zn and Se fluxes estimated by the methods of the deposition on cold substrates and of a quartz crystal monitor.

methods	fluxes (atoms/cm ² sec)	
	Zn	Se
cold substrates	$(3.9 \pm 0.2) \times 10^{14}$	$(2.6 \pm 0.1) \times 10^{14}$
crystal monitor	4.0×10^{14}	2.8×10^{14}

Table 2. Zn and Se fluxes estimated by the methods of the over-flux growth and of a quartz crystal monitor.

methods	fluxes (atoms/cm ² sec)	
	Zn	Se
over-flux growth	$(9.5 \pm 0.4) \times 10^{13}$	$(8.9 \pm 0.2) \times 10^{13}$
crystal monitor	1.02×10^{14}	9.2×10^{13}

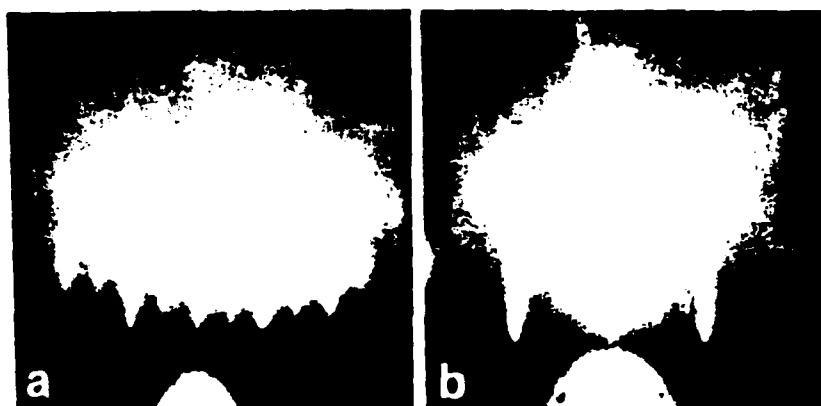


Fig. 1. Reflection high energy electron diffraction (RHEED) patterns taken from the (100) ZnSe grown with the flux ratio of 1.0: (a) [011] and (b) [010] directions.

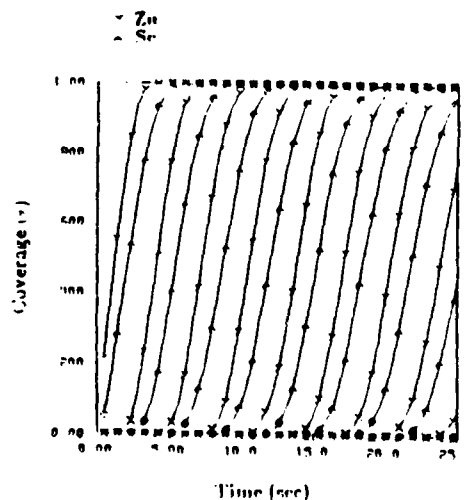


Fig. 2. Coverage profiles of Zn and Se layers of MBE growth of (100) ZnSe as a function of growth time.

Electrical and optical characterization of MBE-grown Ga-doped ZnSe.

M. Vaziri, R. Reifenberger[†], R. L. Gunshor,
L. A. Kolodziejski^{*}, S. Venkatesan, R. F. Pierret.

School of Electrical Engineering
Purdue University, W. Lafayette, IN 47907

[†] Department of Physics, Purdue University.

Abstract

Epitaxial undoped and Ga-doped ZnSe have been grown on (100) GaAs substrates by molecular beam epitaxy (MBE). The optical and electrical properties of these films have been characterized using standard photoluminescence, deep level transient spectroscopy, and transport techniques. For a Zn-to-Se flux ratio of one, the undoped samples exhibit high resistivities; their photoluminescence spectra show a dominant free exciton band edge emission. Under the same growth conditions, low resistivity Ga-doped samples have been produced. The photoluminescence spectra for the doped samples are dominated by bound exciton emission related to the Ga donors (I_2 at 2.795 eV). The deep level transient spectroscopy studies show two prominent defect levels at energies of 0.26 eV and 0.34 eV below the conduction band. Electron transport measurements show that a lightly doped sample having a room temperature carrier concentration of $8.0 \times 10^{14} \text{ cm}^{-3}$ exhibits a peak mobility of $7900 \text{ cm}^2/\text{V.s}$ at 50 K. A higher level of Ga dopant ($n = 1.5 \times 10^{17} \text{ cm}^{-3}$ at room temperature) produces samples with an impurity-band type of conduction at low temperatures.

I. Introduction

ZnSe, a II-IV semiconductor with a direct bandgap of 2.67 eV ($T=300\text{K}$), is an important material for light-emitting devices. Recent growth of pseudomorphic ZnSe on MBE-grown GaAs [1,2] indicates a low interfacial state density can be obtained [3] and suggests that ZnSe is a potentially important candidate for passivation of GaAs devices. In order to satisfy the demands of heterostructure devices, it is essential to have the ability to grow low resistivity ZnSe layers with controlled carrier density and carrier mobility. The growth of thin film ZnSe using MBE techniques offers the possibility of producing high quality material that can be doped in a controlled way. As the quality of source material has improved and the optimal growth conditions have been established, ZnSe can be added to the increasing list of materials that can be successfully grown and doped in an MBE environment.

In this paper we describe the growth and characterization of a number of ZnSe films that have been grown with these goals in mind. We use standard photoluminescence (PL), deep level transient spectroscopy (DLTS), and electronic transport techniques to characterize the optical and electrical properties of the films.

II. Growth of epitaxial layers

The ZnSe epilayers were grown in a Perkin-Elmer model 430 MBE system using elemental sources with a Zn-to-Se flux ratio adjusted to unity (a quartz crystal monitor placed near the sample position measured the flux). All samples were grown at 320 C on semi-insulating (S.I.) GaAs(100) substrates. Observation of the reflection high-energy electron diffraction patterns at various azimuthal angles indicates the growing surface is Se-stabilized. The growth rate is typically 1.2 \AA /s . The source material is zone refined Zn and vacuum

distilled Se supplied by Osaka Asahi Metals.

III. Photoluminescence Result

The PL spectra were measured using a He-Cd laser operating at a wavelength of 3250 Å, a 0.75m SPEX monochromator, and a Hamamatsu GaAs photomultiplier. The excitation power incident on the samples was always below 100 mW/cm². Fig.(1) shows a typical PL spectra of undoped high resistivity ZnSe at T=8 K for two samples with very different thicknesses. The distinctive features in both spectra are the presence of dominant free excitons. The PL spectrum for a thin pseudomorphic ZnSe film grown on a GaAs epilayer (thickness =1000 Å) is shown in Fig. 1a. The free exciton emission peak is split into two peaks at 2.8064 eV and 2.8178 eV. The splitting of the free exciton and the shift to higher energy is a direct consequence of the compressive strain in the pseudomorphic ZnSe epilayer.[1] The compressive strain results from the lattice constant of ZnSe which is .25% larger than that of GaAs. The feature at 2.7997 eV is associated with excitons bound to neutral donors. Fig. 1b shows PL spectra of a 2 μm thick ZnSe epilayer grown on a S.I. GaAs substrate. Several features have been resolved in the band edge emission of this epilayer. The spectra is dominated by a free exciton line at 2.8000 eV and, with more spectral resolution, a feature at 2.8026 eV is also observed. the emission lines at 2.7966 eV and 2.7952 eV are associated with the donor bound excitons and the weak emission at 2.7909 eV (I₁) is related to an exciton bound to neutral acceptors. The origin of the emission line at 2.7952 eV has been subject to controversy [4,9]. Dean et al. [3] argued that this line is a lower energy strain-split component of the I₂ line associated with the Ga donor. Another argument [5,6] is that the line has strong correlation with the stoichiometry and is related to exciton bound to native donors (I_x). A

recent model [9] based on tensile strain resulting from a difference in thermal expansion between ZnSe and GaAs suggests that features in the band edge emission will be split by the same amount. From this model it follows that the peaks at 2.7966 eV and 2.7952 eV are the strain-split components of the I_2 emission line. It also follows that the two features at 2.8000 eV and 2.8026 eV are due to a strain splitting of the free exciton line. However, the 2.6 meV splitting found for the free exciton splitting does not agree with the 1.4 meV splitting found for the I_2 emission feature. This indicates that polariton effects might play a role in splitting the free exciton feature.

In addition and in contrast to Fig. 1a, the band edge emission in Fig. 1b is shifted to lower energy with respect to the emission lines in pseudomorphic ZnSe or their corresponding lines in ZnSe bulk samples. This shift to lower energy for a thick ZnSe epilayer has been observed by other investigators [4,9,10] and can be understood if one assumes that the ZnSe epilayer is under slight biaxial tension originating from a difference in the thermal expansion coefficient between the ZnSe film and the GaAs substrate.

A significant difference between our results and other studies is the presence of a dominant free exciton rather than the bound exciton in band edge emission. This feature is related to the lower level of impurities now available in source materials. As the amount of impurity or dopant increases, the free exciton feature decreases and the bound exciton becomes the dominant feature in the band edge emission. Indeed this was observed for our Ga-doped samples.

For the case of Ga-doped ZnSe, we have selected three representative samples with different amounts of dopant level. The thicknesses of these samples are 2.55 μm , 2.7 μm , and 4.35 μm for samples A, B, and C respectively.

Fig. 2 shows a typical PL spectra from these samples. The presence of sharp and strong excitonic emission and weak emission from donor-acceptor pairs and defect bands (Cu green, SA center) indicate that we have grown good quality Ga-doped ZnSe epilayers. Fig. 3 shows detailed PL spectra in the excitonic region for these samples. The excitonic lines and their energy positions are similar to those observed for the undoped sample in Fig. 1b. The only significant difference is that the dominant feature in the spectra of the Ga-doped samples is now located at 2.795 eV and is associated with a bound exciton line in a thick ZnSe epilayer. It is also clear that as the amount of dopant level increases, the full width at half maximum (FWHM) of the emission line at 2.795 eV becomes larger. Thus it can be concluded that the emission line at 2.795 eV is directly related to the presence of Ga donors in ZnSe epilayers. Also it has been reported that for 4.6 μm ZnSe grown on GaAs, the tensile strain as measured by x-ray and TEM was .04%, yielding a 2 meV splitting between the two valence bands [9]. Fig. 3 clearly shows that the two bound exciton lines for our Ga-doped samples are 2 meV apart. Therefore, it can be concluded that the peaks at 2.795 eV and 2.797 eV are the strain-split components of I_2 line. This interpretation eliminates the possibility of assigning the emission line at 2.795 eV to the native donor (I_1).

IV. Deep Level Transient Spectroscopy

The deep level defects in the Al/ZnSe Schottky diodes were investigated using conventional thermally-scanned deep level transient spectroscopy. Because of the semi-insulating GaAs substrate, a modified dual-Schottky ring-dot structure was used to probe the Ga-doped ZnSe films. DLTS thermal scans were made in the temperature range from 80K to 430K. Sample DLTS data

obtained from the three films of interest are shown in Fig. 4.

As is evident from this figure, each of the three samples exhibit the presence of multiple trap levels. While sample B shows three distinct peaks around 140K, 180K, and 320K, samples A and C clearly display *four* peaks. An additional peak appears around 280K in sample C and near 250K in sample A. The deep level parameters are obtained from an Arrhenius plot of emission rate versus temperature. The activation energies and capture cross-sections deduced from the Arrhenius plots, and the trap concentrations calculated from measured DLTS peak heights for the three samples, are tabulated in Table I. Trap P1 with an activation energy of 0.26eV appears in all three samples and its concentration is a supra-linear function of the doping concentrations. Trap P2 appears in all three samples in small concentrations and is essentially independent of doping.

Previous investigations of ZnSe (both doped and nominally undoped) detected the presence of a trap at 0.34 eV with a capture cross section between 10^{-13} and 10^{-14} cm.². A number of investigators have attributed the presence of this trap to Se vacancies [11,12,13]. We likewise detected the presence of a trap with an activation energy of 0.34 eV below the conduction band edge and with a similar capture cross section. The strong dependence of the trap concentration P1 on doping lends additional credence to the possibility that this trap is associated with the Ga dopant; Myles and Sankey [14] have predicted a deep level in ZnSe due to gallium-on-zinc-site complexed with a Se vacancy (Ga_{Zn}, V_{Se}) at an activation energy of approximately 0.28 eV.

In addition to the traps P1 and P2, common to all three samples, sample A shows the presence of large concentrations of traps P3 and P7 which are *absent* in samples B and C. Moreover, the sample A trap concentrations are

more than an order of magnitude larger than the trap concentrations in samples B and C. The origin of these traps is not known, though it is possible that the traps are related to impurities incorporated into the ZnSe films along with the Ga dopant.

V. Transport results

For transport measurements, ohmic contacts were made using a Hg-In alloy followed by a 290 C anneal in forming gas for 3 to 4 minutes. All contacts remain ohmic even at low temperatures. The temperature dependence of the Hall effect and resistivity were measured in a Van der Pauw configuration using a Model 1808 Keithley Hall package.

An attempt to measure the resistivity of undoped samples failed and indications are that the sample resistivity was high ($\rho > 10^5 \Omega\text{-cm}$). Thus, due to shunting of the sample by the substrate, more precise results could not be obtained.

For Ga-doped samples the resistivity, mobility, carrier concentration, and Hall coefficient have been measured as a function of temperature. Fig. (5) shows a semilog plot of the resistivity versus inverse temperature. The initial reduction in resistivity with decreasing temperature is due to a reduction in phonon scattering. Further reduction in temperature leads to a gradual freezing out of donor electrons which results in an increase in the resistivity. The slope of $\log_e \rho$ vs. $1/T$ in this freeze out region gives an activation energy ϵ_1 which is close to the ionization energy for an isolated Ga donor [15]. The values of ϵ_1 for samples A, B, and C extracted from Fig. 5 are 15.5 ± 1 meV, 26.5 ± 1 meV, and 27.0 ± 1 meV respectively.

The temperature dependence of the carrier concentration in these materials enables one to estimate the number of donors (N_D) and acceptors (N_A) as well as the ionization energy (E_D) for the conduction electrons. Fig. 6 shows the carrier concentration (n) as function of temperature for the three Ga-doped samples. The carrier concentrations were calculated from the measured Hall coefficient R_H and the Hall factor r assumed equal to unity. In order to analyze the data the well-known formula for non-degenerate statistics was used [16]:

$$\frac{n(n+N_A)}{(N_D-N_A-n)} = N_c / g \exp(-E_D/kT) \quad (1)$$

In Eq. 1 N_c is the density of states in the conduction band and is given by $2(2\pi m^* kT)^{1.5}$. The electron effective mass of $m^* = .17m_0$ and the degeneracy factor $g=2$ were also used. The solid lines through the experimental points represent the best fit of Eq. 1 to the data. The parameters used in obtaining the fit for both samples B and C are given in the figure caption. This standard form of analysis is found to be inappropriate for sample A, which contains a higher level of Ga dopant.

The temperature dependence of the electron mobility also provides useful information about the scattering mechanism in these materials. Fig. 7 shows the temperature dependence of the Hall mobility for these Ga-doped samples. The room temperature mobilities of these samples are around $400 \text{ cm}^2/\text{V.s}$ which is close to the calculated value for polar optical phonon scattering ($550 \text{ cm}^2/\text{V.s}$). As the temperature decreases the mobility for both samples B and C increases, reaching a maximum value around 50 K. As the temperature further decreases the mobility decreases due to ionized impurity scattering. The peak mobility of $7900 \text{ cm}^2/\text{V.s}$ at 50 K was obtained for sample C; this is

the highest value reported for an intentionally doped ZnSe film.

It is important to notice that the temperature dependence of the resistivity, carrier concentration, and mobility of sample A is quite different than the other samples studied. In particular, at low temperature these differences become more pronounced. For example, at liquid helium temperatures, the mobility of this sample is very low (around $1 \text{ cm}^2/\text{V.s}$) and a plot of $\log \rho$ vs. $1/T$ shows an additional activation energy of about 2 meV. The temperature dependence of the Hall coefficient for this sample exhibits a sharp peak at $T = 38 \text{ K}$. These observations may indicate a change in conduction mechanism from free carriers to impurity-band conduction for this sample.

V. Summary

Epitaxial layers of undoped and Ga-doped ZnSe have been grown on (100) GaAs substrates by molecular beam epitaxy. The observed PL spectra of undoped pseudomorphic and thick ZnSe epilayers indicate that the dominant feature in the band edge emission is related to free excitons. In contrast to the results of investigators using source material of lesser purity, the resistivity of the undoped sample is very high for $J_{\text{Zn}}/J_{\text{Se}} \approx 1$. This indicates that our elemental source materials and MBE system introduce low levels of impurities, a factor which is essential for the doping process to be successful in this material.

The PL spectra of Ga doped samples has a dominant feature at 2.795 eV (I_2). The FWHM of this feature increases as the amount of Ga dopant increases. From the comparison of PL spectra for undoped and Ga-doped samples, it was concluded that the 2.795 eV line is the strain split component of the I_2 line and not that of a native donor. The DLTS measurements show two

prominent defect levels. The deep level at 0.26 eV below the conduction band is tentatively identified as a $(\text{Ga}_{\text{Zn}}, \text{V}_{\text{Se}})$ dopant site complex and the trap with an activation energy of 0.34 eV is attributed to native defects arising from Se vacancies in the ZnSe films. The resistivity and the Hall effect were also measured and a peak mobility of $7900 \text{ cm}^2/\text{V.s}$ was obtained. The sample with a high level of Ga dopant behaves differently and impurity-band conduction may take place at low temperatures.

Acknowledgements

The authors would like to thank D. Lubelski, R. Holzer, and J. Qiu for their contributions to this work. Research support was provided by a Defense Advanced Research Projects Agency/Office of Naval Research University Research Initiative Program N00014-86-K0760 and by, Air Force Office of Scientific Research grant No. 85-0185, Office of Naval Research contracts N00014-86-K-0378 and N00014-87-K0522, and by the Indiana Corporation for Science and Technology Grant No. P-5058.

References

- * Present address, Department of Electrical Engineering and Computer Science, Massachusetts Institute of Technology, Cambridge, MA 02139.
1. R. L. Gunshor, L. A. Kolodziejski, M. R. Melloch, M. Vaziri, C. Choi, and N. Otsuka. *Appl. Phys. Lett.*, **50**, 200(1987).
 2. G. D. Studtmann, R. L. Gunshor, L. A. Kolodziejski, M. R. Melloch, J.A. Cooper, Jr., R. F. Pierret, D. P. Munich, C. Choi, and N. Otsuka. *Appl. Phys. Lett.*, **52**, 1249(1988).
 3. Q-D. Qian, J. Qiu, J. L. Glenn, Sungki O, R. L. Gunshor, L. A. Kolodziejski, M. Kobayashi, N. Otsuka, M. R. Mollock, J. A. Cooper, Jr., M. Haggerott, T. Heyen, and A. V. Nurmikko, *Proc. 5th Int. Conf. on Molecular Beam Epitaxy*, Sapporo, Aug. 1988, to appear in *J. Crystal Growth*.
 4. P. J. Dean, A. D. Pitt, P. J. Wright, M. Young, and B. Cockayne, *Physica* **116B**, 508(1983).
 5. T. Yao, Y. Makita and S. Maekawa, *Jpn. J. Appl. Phys.*, **20**, L741(1981).
 6. T. Yao, T. Takeda, and R. Watanuki, *Appl. Phys. Lett.*, **48**, 1615(1986).
 7. J. E. Potts, H. Cheng, S. Mohapatra, and T. L. Smith, *J. Appl. Phys.*, **61**, 333(1987).
 8. K. Mohammed, D. A. Cammack, R. Dalby, P. Newbury, B. L. Greenburg, J. Petruzzello, and R. N. Bhargava, *Appl. Phys. Lett.*, **50**, 37(1987).
 9. Khalid Shahzad, to be published in *Phys. Rev. B*.
 10. T. Yao, Y. Okada, S. Matsui, K. Ishida, and I. Fujimoto, *J. Crystal Growth*, **81**, 518(1987).

11. K. A. Christianson and B.W. Wessels, J. Appl. Phys. 54, 4205 (1983).
12. P. Besomi and B.W. Wessels, J. Appl. Phys. 53, 3076 (1982).
13. Y. Shirakawa and H. Kukimoto, J. Appl. Phys. 51, 5859 (1980).
14. C. W. Myles and O.F. Sankey, Phys. Rev. B29, 6810 (1984).
15. B. I. Shklovskii and A. L. Efros, "Electronic Properties of Doped Semiconductors", edited by M. Cardona (Springer-Verlag, Berlin, 1984) P 76.
16. M. Aven, J. Appl. Phys., 42, 1204(1971).

Figure Captions

Figure 1: The low temperature band edge photoluminescence of undoped ZnSe epilayers with different thicknesses is dominated by free exciton emission.

Figure 2: The low temperature photoluminescence of Ga-doped ZnSe films. The room temperature carrier concentration for the three samples are (A) $1.5 \times 10^{17} \text{ cm}^{-3}$, (B) $5.2 \times 10^{15} \text{ cm}^{-3}$, and (C) $8.0 \times 10^{14} \text{ cm}^{-3}$. R is the ratio of band edge emission intensity to the defect band intensity. (The spurious feature at 650nm is due to the incident laser line).

Figure 3: The low temperature band edge photoluminescence of three Ga-doped ZnSe epilayers. The room temperature carrier concentration for the three samples are (A) $1.5 \times 10^{17} \text{ cm}^{-3}$, (B) $5.2 \times 10^{15} \text{ cm}^{-3}$, and (C) $8.0 \times 10^{14} \text{ cm}^{-3}$.

Figure 4: The DLTS spectra of three different Ga-doped ZnSe epilayers. The activation energies, capture cross sections and trap concentrations for each trap are listed in Table 1.

Figure 5: The temperature dependence of the resistivity for three different levels of Ga doping in ZnSe epilayers. The activation energy of the Ga dopant in each sample is (A) $15.5 \pm 1 \text{ meV}$, (B) $26.5 \pm 1 \text{ meV}$, and (C) 27.0 ± 1 .

Figure 6: The temperature dependence of the carrier concentration for three different levels of Ga doping in ZnSe epilayers. The solid line is a result of least squares fitting to Eq. 1 given in the text. The fitting parameters are (B): $N_D = 8.3 \times 10^{15} \text{ cm}^{-3}$, $N_A = 5.0 \times 10^{15} \text{ cm}^{-3}$, $E_D = 20 \text{ meV}$; (C): $N_D = 2.1 \times 10^{15} \text{ cm}^{-3}$, $N_A = 1.4 \times 10^{15} \text{ cm}^{-3}$, $E_D = 22 \text{ meV}$.

Figure 7: The temperature dependence of the mobility for three different levels of Ga doping in ZnSe epilayers. The peak mobility found in this study is $7900 \text{ cm}^2/\text{V.s}$ at 50K. The room temperature carrier concentration for the three samples are (A) $1.5 \times 10^{17} \text{ cm}^{-3}$, (B) $5.2 \times 10^{15} \text{ cm}^{-3}$, and (C) $8.0 \times 10^{14} \text{ cm}^{-3}$.

Table 1: The activation energy, capture cross section and trap concentration for the deep level traps found in three different Ga doped ZnSe epilayers.

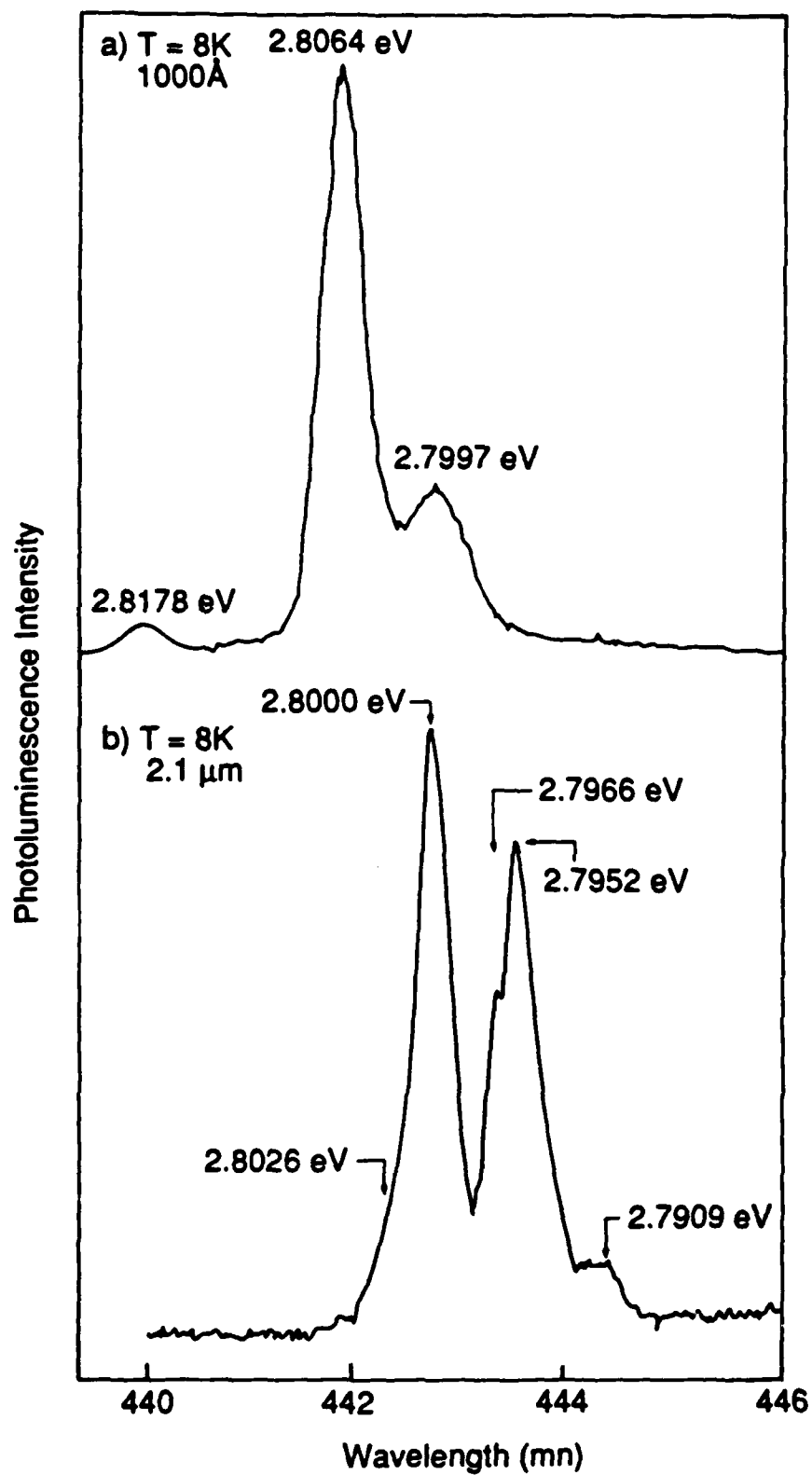


Fig. (1)

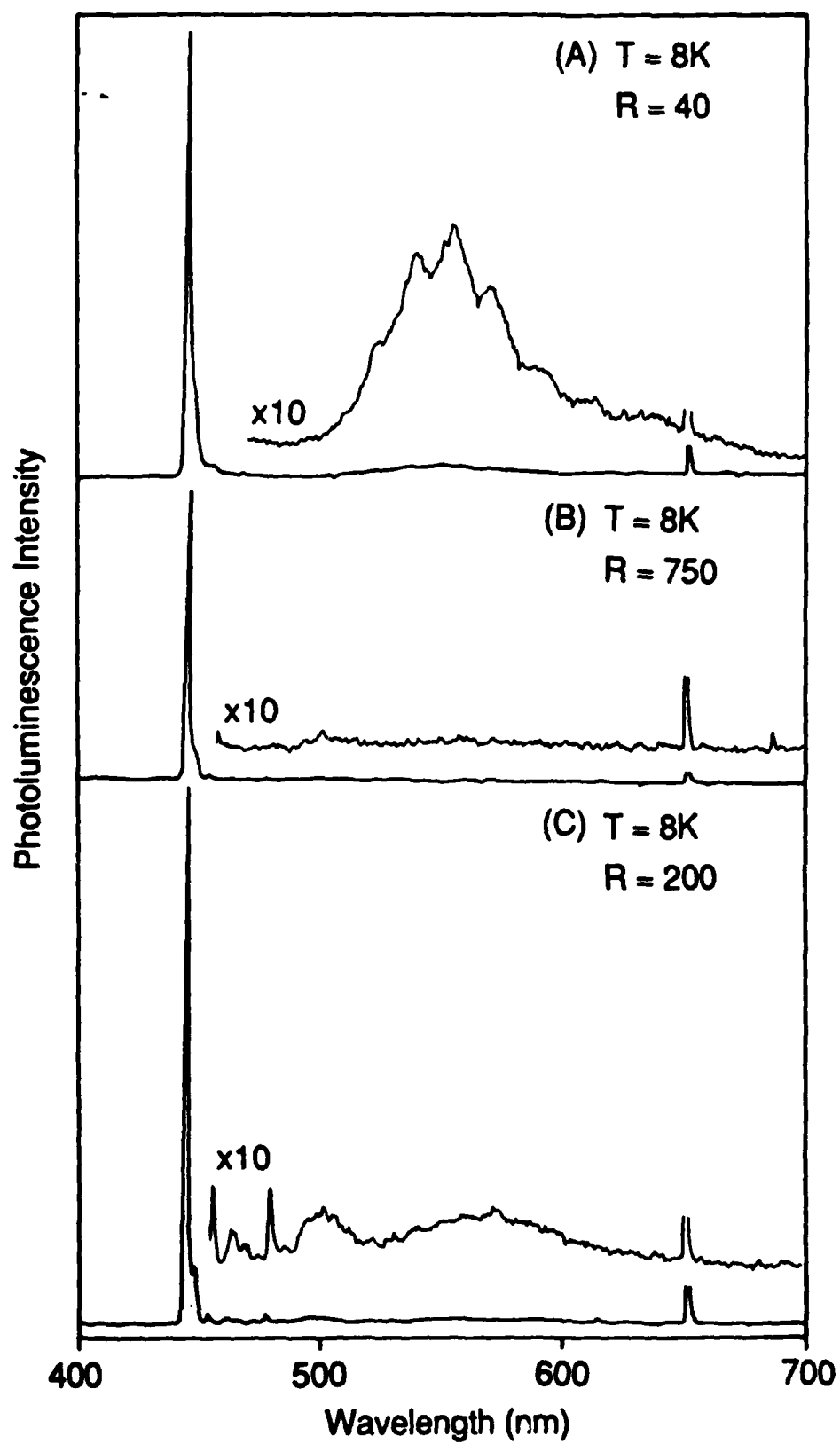


Fig. (2)

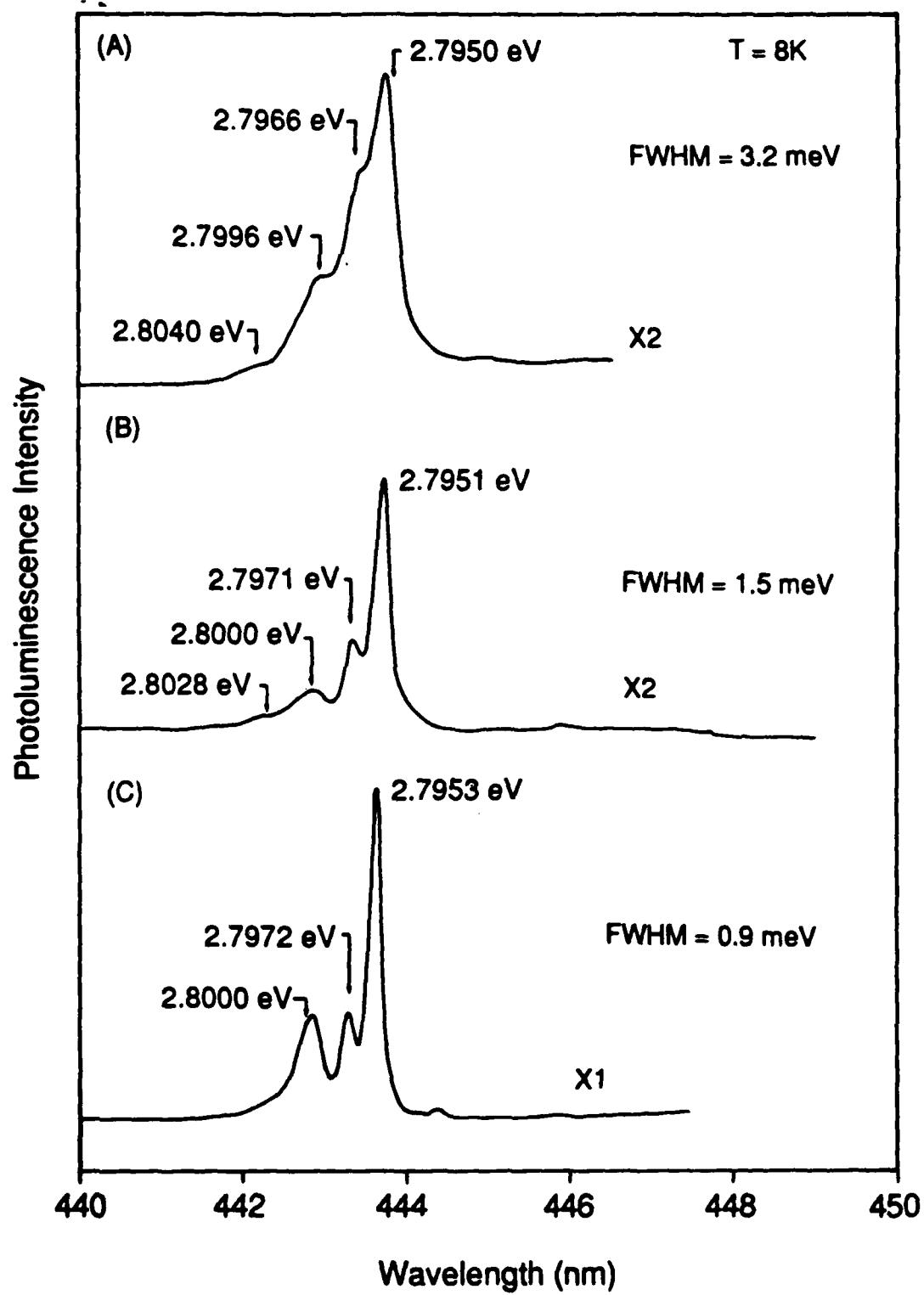


Fig. (3)

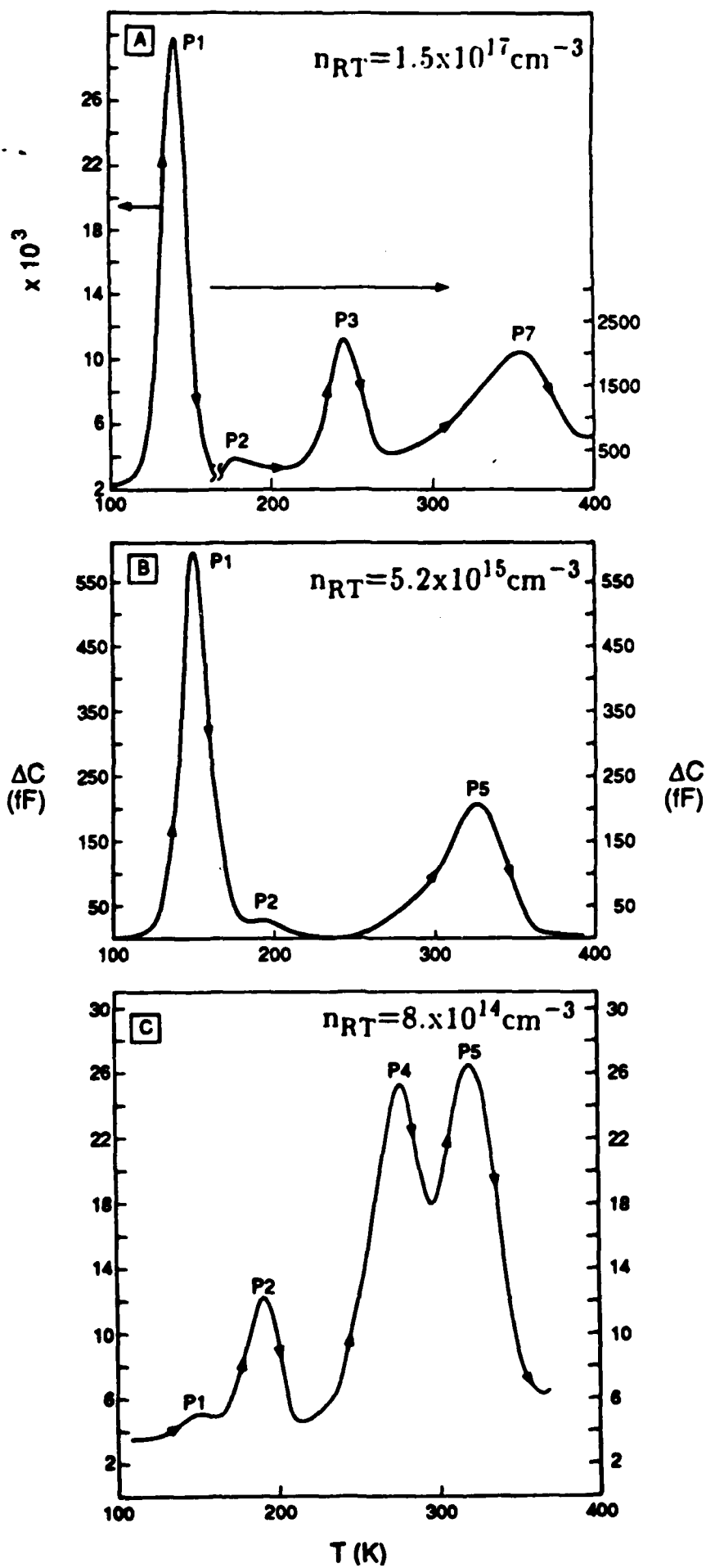


Fig. (4)

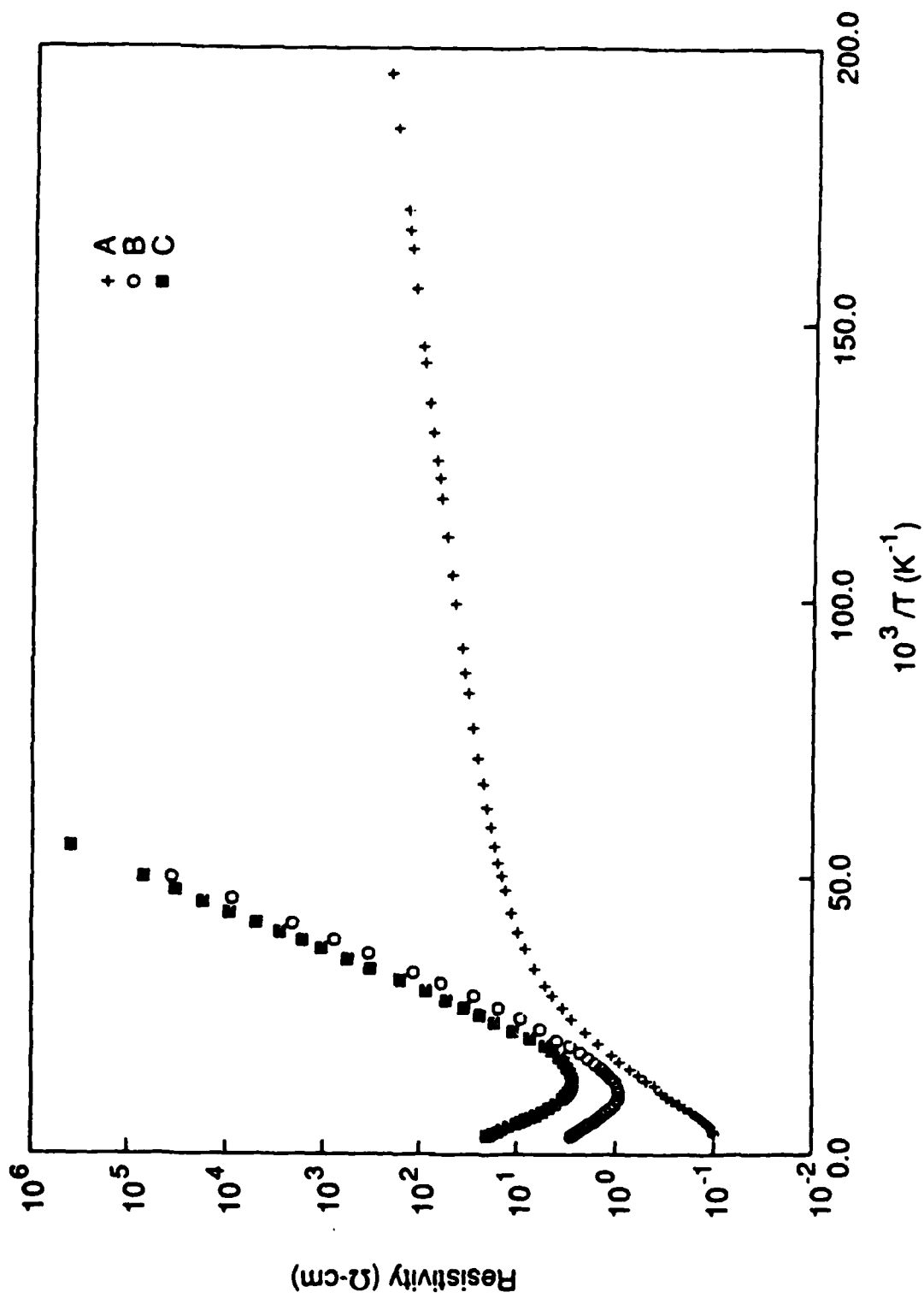


Fig. (b)

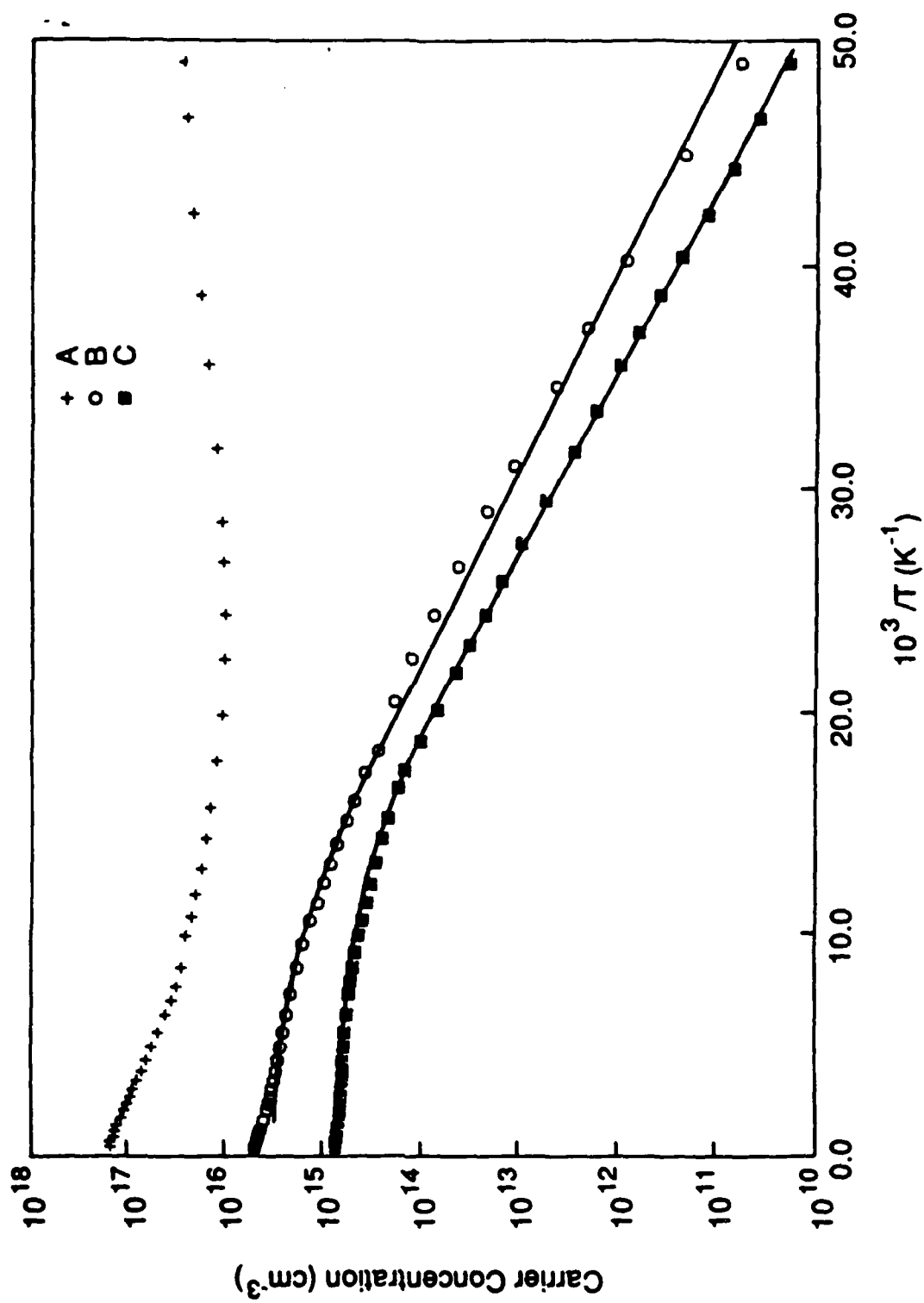


Fig. (6)

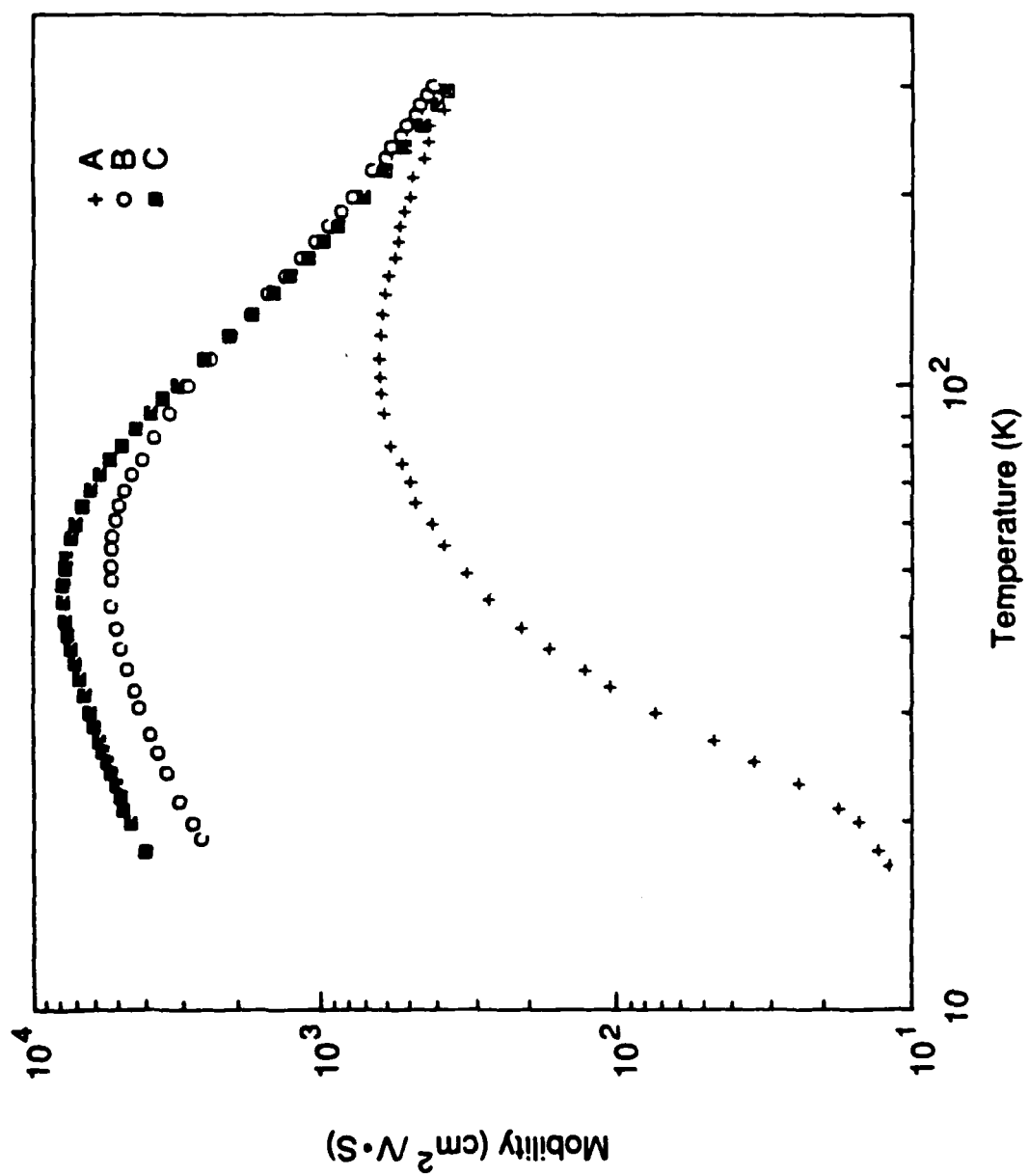


Fig. (7)

Trap P 1			
	ΔE (eV)	σ_n (cm ²)	Trap Conc.(cm ³)
Sample A	0.26 ± 0.02	3 x 10 ⁻¹⁴	3.4 x 10 ¹⁷
Sample B		6 x 10 ⁻¹⁴	1.9 x 10 ¹⁵
Sample C		1 x 10 ⁻¹³	5.9 x 10 ¹²
Trap P2			
Sample A	0.34 ± 0.04	-	8.8 x 10 ¹⁴ est
Sample B		3 x 10 ⁻¹³	1.5 x 10 ¹³ est
Sample C		3 x 10 ⁻¹⁵	1.5 x 10 ¹³
Trap P3			
Sample A	0.48	1 x 10 ⁻¹³	3.6 x 10 ¹⁶
Trap P4			
Sample C	0.47	6 x 10 ⁻¹⁵	3.6 x 10 ¹³
Trap P5			
Sample B	0.53 ± 0.05	6 x 10 ⁻¹⁶	4.8 x 10 ¹⁴
Sample C		2 x 10 ⁻¹⁴	4.1 x 10 ¹³
Trap P7			
Sample A	0.67	9 x 10 ⁻¹⁵	2.3 x 10 ¹⁶

est : indicates estimated values

Excitonic trapping from atomic layer epitaxial ZnTe within ZnSe/(Zn,Mn)Se heterostructures

L. A. Kolodziejski and R. L. Gunshor

School of Electrical Engineering, Purdue University, West Lafayette, Indiana 47907

Q. Fu, D. Lee, and A. V. Nurmikko

Division of Engineering and Department of Physics, Brown University, Providence, Rhode Island 02912

J. M. Gonsalves and N. Otsuka

Materials Engineering, Purdue University, West Lafayette, Indiana 47907

(Received 30 October 1987; accepted for publication 27 January 1988)

ZnSe-based structures have been fabricated, consisting of monolayers of ZnTe grown by atomic layer epitaxy spaced by appropriate dimensions to approximate a Zn(Se,Te) mixed crystal; this method has been used to overcome the difficulties encountered in the molecular beam epitaxy (MBE) of the alloy with a low Te concentration. Reported work has shown that blue-blue/green luminescence, originating from exciton self-trapping at Te sites in Zn(Se,Te) bulk crystal alloys, is significantly more intense than the light emitted from ZnSe. Luminescence originating from ZnTe-containing ZnSe/ZnTe superlattice and ZnSe/(Zn,Mn)Se multiple quantum well structures was used to illustrate how the presence of ZnTe acts to trap excitons. Optical signatures of the MBE-grown structures were similar to those of the random alloy, indicating that the exciton self-trapping mechanism is important to the interpretation of recombination processes in structures containing ZnSe/ZnTe heterointerfaces.

Epitaxial layers, superlattices, and multiple quantum well structures involving wide band-gap semiconductors such as ZnSe and ZnTe are of current interest for optical device applications in the blue and blue-green regions of the spectrum. Alloying ZnSe with Te to form Zn(Se,Te) permits adjustment of the lattice constant, and a lowering of the band gap (roughly from 2.8 to 2.4 eV), and provides opportunities for amphoteric doping. Of particular interest is the observation that the photoluminescence yield of Zn(Se,Te) can be significantly enhanced over that of bulk ZnSe crystals^{1,2} and epitaxial layers above liquid-helium temperatures due to localization of excitons in the random alloy. In this letter we describe the fabrication and selected optical properties of a new approach to provide versatile ZnSe-ZnTe microstructures which combine benefits of both a superlattice and a bulk alloy.

The growth of the Zn(Se,Te) mixed crystal by molecular beam epitaxy is complicated by a difficulty in controlling the composition. In the work reported by Yao *et al.*,³ over the entire range of Te fraction, a three to ten overpressure of Te was required. In our laboratory we have grown a number of Zn(Se,Te) epilayers with varying fractions of Te; a particular difficulty was encountered when a small fraction of Te was desired (< 10%), resulting in widely varying compositions under what appeared to be similar growth conditions. To circumvent the problems associated with controlling the alloy concentrations, we have designed ZnSe-based structures consisting of ultrathin layers (or "sheets") of ZnTe spaced by appropriate dimensions to approximate a Zn(Se,Te) mixed crystal with low or moderate Te composition. In one case, such a "pseudo-alloy" was grown as an epilayer consisting of a 100-period superlattice with each period containing one monolayer of ZnTe (~ 3 Å) separated by 100 Å of ZnSe. In a second prototype structure, the pseudo-alloy was used to modify the ZnSe quantum well in a

ZnSe/Zn_{0.8}Mn_{0.2}Se heterostructure. In such multiple quantum well (MQW) structures either one or two ZnTe sheets were placed in the center of each ZnSe well; the wells had thicknesses ranging from 44 to 130 Å. The lattice mismatch between bulk ZnSe and ZnTe is approximately 7.4%; in these circumstances the ZnTe sheets are likely to accommodate most of the strain. Although the architecture of these structures was substantially different from each other as well as from a bulk alloy, their optical signatures (photoluminescence) were dominated by similar features which were also found in the bulk alloy crystals at low to moderate Te composition. We show below, by using one of our novel structures as an illustration, how the dominant luminescence originates from highly efficient capture of excitons at the ZnSe-ZnTe heterointerfaces, a process which is most probably intrinsic to the quasi-two-dimensional pseudo-alloys as well as the mixed crystal bulk case studied earlier.²

The structures described above were fabricated by a combination of molecular beam epitaxy (MBE) and atomic layer epitaxy (ALE) techniques using a Perkin-Elmer model 430 MBE system. GaAs (100) substrates were used and were chemically prepared in the conventional manner.⁴ During the growth of the ZnSe material, the fluxes of Zn and Se were set to be equal as measured by a quartz crystal monitor and the substrate temperature was maintained at 320 °C. Following the deposition of a 1–2-μm-thick ZnSe buffer layer, a multiple quantum well [with (Zn,Mn)Se barrier layers] or a superlattice of ZnSe/ZnTe was grown by the MBE growth technique but interrupted for the ALE growth of the ZnTe monolayer sheets. In an effort to optimize the interface abruptness of the ZnTe monolayer, the ALE of ZnTe was performed on a recovered ZnSe surface which made up, for example, the first half of a quantum well. The ALE growth involved the following sequence of shutter operation (which included appropriate desorption times after each depo-

sition): (1) Zn, (2) Te, (3) Zn, and (4) Se. The second half of each quantum well was continued by MBE of ZnSe. Reflection high-energy electron diffraction (RHEED) was used to monitor the surface structure during growth. After recovery of each Zn, Te, or Se surface we observed the expected Zn-stabilized, Te-stabilized, or Se-stabilized reconstructed surface, respectively, in agreement with the observations reported by Yao and Toshihiko.⁵

The pseudo-alloy structures have been examined by cross-sectional transmission electron microscopy (TEM). Clear images of ultrathin ZnTe sheets were observed in dark field images of the (200) reflection. These ultrathin sheets appeared as narrow bright lines with widths of about 5 Å in the dark field images, indicating the existence of continuous ZnTe monolayers in ZnSe crystals. Although Xe ions were used for the final thinning of cross-sectional samples, superlattice areas have suffered some damage. Because of the damage and the lower resolution of the dark field imaging technique, details of ZnSe-ZnTe heterointerfaces could not be seen in the images. However, the TEM observation has clearly shown that ZnTe sheets have formed coherent interfaces with ZnSe layers.

Initial optical characterization of these structures has been made through luminescence studies. For comparison purposes, Fig. 1(a) shows the low-temperature photoluminescence spectrum of a "conventional" ZnSe/(Zn,Mn)Se MQW structure in the absence of any ZnTe, excited by a low-power continuous-wave dye laser. The sample had a ZnSe well thickness of 65 Å with a Mn concentration in the barrier of $x = 0.23$. The luminescence is dominated by the sharp (< 5 meV), bright, blue exciton recombination at the $n = 1$ (light hole) quantum well transition. [A summary of optical properties of ZnSe/(Zn,Mn)Se quantum wells can be found in Ref. 4.] The efficiency of collection of photoexcited electron hole pairs into the ZnSe wells is demonstrated by the dominance of the exciton recombination radiation over the yellow luminescence from the Mn-ion internal tran-

sitions, the latter of which can be very effectively excited in (Zn,Mn)Se bulk epitaxial material. As a striking contrast to Fig. 1(a), the photoluminescence from a ZnSe/(Zn,Mn)Se MQW which now incorporates the ZnTe sheets inserted into each quantum well is shown in Fig. 1(b). For this structure the ZnSe well width was approximately 44 Å as measured by TEM. The luminescence in this instance exhibits two broad emission bands with half-widths on the order of 50 and 100 meV with peak positions approximately 100 and 300 meV below the band-edge region, respectively. In the following we denote the two bands as S_1 and S_2 , respectively, following the notation of Ref. 2. The high-energy edge of band S_1 shows additional modulation; this is due to phonon sidebands of excitons bound to impurities in the ZnSe well and/or buffer layer. [The raw data also included Fabry-Perot oscillations in our thin-film samples which for clarity have been mathematically averaged out in Fig. 1(b).] The spectrally integrated luminescence yield at $T = 2$ K for both quantum well samples in Fig. 1 was comparable; however, that for the sample without ZnTe sheets decreased precipitously with increasing temperature. The location of the absorption edge in this quantum well sample was established through photoluminescence excitation spectroscopy, a relevant portion of which is shown in Fig. 1(c). The spectral position of the distinct $n = 1$ light hole exciton resonance indicates that the addition of the ultrathin ZnTe layers does not significantly shift the position of this lowest energy transition; this is readily verified by comparing the excitation spectra of the sample without ZnTe.⁶ While band offset information about the ZnSe/ZnTe heterojunction is not yet available, electron affinity data suggest that the ZnTe layer would provide a narrow additional potential well in the valence band of depth as much as 1 eV while contributing to a thin barrier in the conduction band of some 0.6 eV in height. One difference between the excitation spectra of the MQW structures with and without the ZnTe layers was the somewhat broader low-energy tail for the former. Spectra similar to that in Fig. 1(b) were observed for a number of samples containing sheets of ZnTe in quantum wells of ZnSe with thicknesses ranging from 44 to 130 Å. Similar spectra (showing the S_1 and S_2 bands) were also observed for the pseudo-alloy structure composed of a ZnSe/ZnTe superlattice with one period having monolayer sheets of ZnTe spaced by 100 Å of ZnSe.

We have also examined the temperature dependence (Fig. 2) of the luminescence spectra in the pseudo-alloy structures. While the details will be described elsewhere, we note that for the sample of Fig. 1(b) two distinct temperature regions were observed. Starting from a low temperature the emission band S_1 is first quenched; this occurs quite precipitously in a fairly narrow temperature range of $T = 70$ – 90 K. Second, at temperatures beyond $T = 120$ K, or so, a strong spectral red shift is seen for the remaining S_2 luminescence but with decreasing quantum efficiency. This shift is much larger than a simple band-gap reduction and indicates that the partial quenching of the emission band S_2 brings yet additional lower energy band(s) into view.

These results can be compared with recent work which has shown how exciton self-trapping is a very efficient pro-

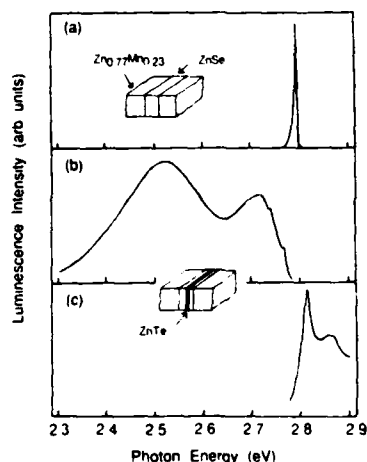


FIG. 1. Comparison of photoluminescence spectra at $T = 2$ K of a ZnSe/(Zn,Mn)Se MQW sample (a), with that of a similar structure but with the insertion of monolayer sheets of ZnTe in the middle of the quantum well (b). [The amplitude of emission in (a) has been reduced to bring the peak to scale.] The photoluminescence excitation spectra of sample (b) is shown in the bottom panel (c). In both cases the yellow Mn-ion internal emission was significantly below that from the blue-green region.

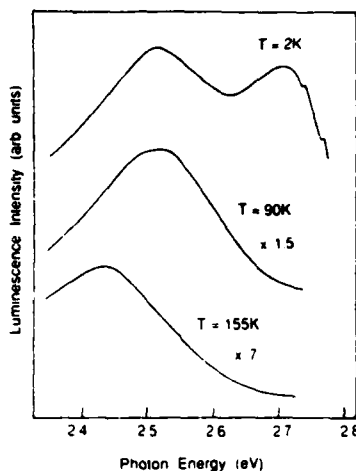


FIG. 2. Photoluminescence from the ZnSe/(Zn,Mn)Se MQW sample with ZnTe sheets shown as a function of temperature.

cess in bulk Zn(Se,Te) alloys where it is characterized by broad emission lines and large Stokes shifts relative to the fundamental absorption edge.² In particular, the emission bands S_1 and S_2 have been interpreted with trapping and strong accompanying local lattice relaxation about single and double Te sites, respectively. In a bulk crystal of low Te concentration ($x < 0.05$), exciton recombination from the S_1 band dominates at low temperature but is partially quenched at higher temperatures. This occurs as a consequence of excitons in traps associated with emission S_1 first obtaining sufficient thermal energy to reach over a potential barrier for their localization, the process being activated in a narrow temperature range very similar to that observed in the present case. However, the initial dominance of the S_2 band at low temperatures and the emergence of other red-shifted emission features suggest a more complex trapping process in the ZnSe-ZnTe pseudo-alloy than encountered in the case of a dilute bulk Zn(Se,Te) mixed crystal.

In the modified quantum well structures considered here, the process leading to recombination spectra such as in Fig. 1(b) is then interpreted as follows. Initial photoexcitation of electron hole pairs is followed by rapid thermalization of the carriers within the ZnSe quantum wells. However, before any substantial exciton recombination across the superlattice band gap takes place, their capture at the ultrathin ZnTe layers at the middle of the wells occurs with simultaneous local lattice relaxation and subsequent strong radiative recombination at optimally located Te sites. We do not have any direct measurement of the trapping times, but typical exciton lifetime of ~ 100 – 200 ps in the ZnSe/(Zn,Mn)Se quantum wells has been obtained through time-resolved luminescence experiments.⁷ Furthermore, while the microscopic details of the trapping are not fully known, it is most likely that the capture is dominated by the hole part of the exciton; i.e., driven by the hole-phonon interaction at the isoelectronic Te traps.

A question which is raised by these observations concerns the "sharpness" of the ZnSe/ZnTe interface, i.e., to what degree is interdiffusion of the anions necessary to provide a finite mixed crystal region compatible for the trapping scenario described above. Alternatively, approaching the

question from the perspective of the two-dimensional growth aspect in atomic layer epitaxy, we may ask how much do the ZnTe layers deviate from an ideally complete monolayer. In this letter we cannot yet provide a quantitative answer; however, since the largest contribution to luminescence at low temperature is already by the emission band S_2 (and not S_1 as in a dilute bulk mixed crystal), and since there is the additional clear emergence of lower emission bands at temperatures above 120 K (Fig. 2), we can qualitatively conclude that pairs of Te isoelectronic traps as well as more complicated clusters are more numerous than single isolated Te lattice sites. Starting from an initially perfect monolayer of ZnTe this implies that interdiffusion would be very unlikely to extend over much more than a molecular monolayer (~ 3 Å) in our structures; otherwise, within the resulting inhomogeneous Zn(Se,Te) interface region the density of single Te sites would dominate. Work is presently under way to reach a more precise answer on this issue, including the possible influence of the large lattice mismatch strain in the ZnTe layers on the microscopic details of the heterointerface.

In summary, we have designed and tested ZnSe quantum well structures which show quite dramatically the strong exciton capture at a ZnSe/ZnTe interface where there is perhaps only a little (but yet a finite amount of) interdiffusion or related compositional disorder. The self-trapping of excitons at Te sites is likely to dominate the recombination process in ZnSe/ZnTe superlattices⁸ composed of thin (\sim monolayer) ZnTe alternated with thicker ZnSe layers. Furthermore, it is expected that the self-trapping phenomenon plays a role in the radiative processes of a variety of structures containing the ZnSe/ZnTe heterointerface. At the same time, the capture process discussed here may be useful in enhancing the quantum efficiency in superlattices at noncryogenic temperatures where defects might otherwise limit luminescence from free or weakly bound excitons.

The authors would like to acknowledge the following people for their contributions to this work: M. Vaziri, D. Lubelski, C. Choi, R. Holzer, and J. Glenn. The research at Purdue and Brown was supported by a joint Defense Advanced Research Projects Agency/Office of Naval Research University Research Initiative Program N00014-86-K0760. Additional support was provided to Purdue by Office of Naval Research contract N00014-82-K0653 and National Science Foundation-MRG grant DMR-8520866. Additional support to Brown was provided by Office of Naval Research contract N00014-83-K0638.

¹A. Reznitsky, S. Permogorov, S. Verbin, A. Naumov, Yu. Korostelin, and S. Prokov'ev, *Solid State Commun.* **52**, 13 (1984).

²D. Lee, A. Mysyrowicz, A. V. Nurmikko, and B. J. Fitzpatrick, *Phys. Rev. Lett.* **58**, 1475 (1987).

³T. Yao, Y. Makita, and S. Maekawa, *J. Cryst. Growth* **45**, 309 (1978).

⁴L. A. Kolodziejski, R. L. Gunshor, N. Otsuka, S. Datta, W. M. Becker, and A. V. Nurmikko, *IEEE J. Quantum Electron.* **QE-22**, 1666 (1986).

⁵T. Yao and Y. Toshihiko, *Appl. Phys. Lett.* **48**, 160 (1986).

⁶Y. Hefetz, J. Nakahara, A. V. Nurmikko, L. A. Kolodziejski, R. L. Gunshor, and S. Datta, *Appl. Phys. Lett.* **47**, 989 (1985).

⁷Y. Hefetz, J. Nakahara, A. V. Nurmikko, L. A. Kolodziejski, R. L. Gunshor, and S. Datta, *Appl. Phys. Lett.* **48**, 372 (1985).

⁸See, e.g., H. Fujiyasu, K. Mochizuki, Y. Yamazaki, M. Aoki, and A. Sasaki, *Surf. Sci.* **174**, 542 (1986); M. Kobayashi, N. Mino, H. Katagiri, R. Kimura, M. Konagai, and K. Takahashi, *Appl. Phys. Lett.* **48**, 296 (1986).